Image-source method and truncation of a series expansion of the integral solution - Case of an angular sector in 2D

Running title: Ray method compared to integral solution

Vincent Martin

CNRS - Laboratoire de Mécanique Physique, 2, place de la Gare de Ceinture,

F-78210 St-Cyr l'Ecole, France, vmartin@ccr.jussieu.fr

Thomas Guignard

EPFL – Laboratoire d'Electromagnétisme et d'Acoustique, STI-ITOP-LEMA, Station11,

CH-1015 Lausanne, Switzerland, thomas.guignard@epfl.ch

Abstract - The acoustic ray method rests upon specular reflection, an intuition that gives access only to an approximation of the solution by not taking into account the parts of the field called diffusion and diffraction. In trying to understand rationally the roots of the approximation, it has appeared that the image source could be generalized and also that errors may be partially due to missing generalized sources, already in elementary geometries such as obtuse angles. Indeed, it is shown that the exact integral solution of a 2D acoustic problem, expressed as a series of terms, could be seen as the contribution of the different image sources, via a partial use of the Huygens' Principle. With the correspondence between the terms and the image sources shown, the missing sources would appear and the method would thereby be refined.

PACS numbers: 43.20.Dk

I – INTRODUCTION

In acoustic cavities such as concert halls or passengers' spaces in vehicles, the numerical description of classical sound fields – those satisfying the Helmholtz equation in space-frequency domain with local boundary conditions – stems from various methods, the choice of which depends first of all on the ratio of the wavelength to a linear dimension of the considered cavity. The reasons for this choice are either of conceptual or practical nature and each method has its own advantages and drawbacks. For example, the boundary finite element method, developed from the exact integral representation of the Helmholtz operator solution, is impractical for high frequencies, as the necessary fine discretization of the boundaries would then lead to large and full matrices, taking a long time to build and inverse. In the adequate frequency range, the method cannot be extended to non-linear problems (at least not directly). It needs knowledge of the acoustic field everywhere on the boundaries before giving access to the field at the points of interest inside the domain.

The finite element method (finite elements of volume), resting on the variational form stemming from the weak form of the equation under study, is also confined to sufficiently long wavelengths for the same practical reasons of discretization, this time of the domain, even if the matrices are more quickly built and inversed as they can be made with a large number of null terms. As an indication, it is not easy to describe sound fields in the audible medium frequency range (1kHz - 5kHz) in passengers' space in aircrafts, helicopters, cars, etc... The method is appropriate for non-linear problems. It necessarily describes the field everywhere within the domain and on the boundaries (substructuration could lead directly to the boundary values but at the expense of supplementary calculation time).

As for the ray method, it is restricted to the description of fields arising from specular reflections and does not take diffraction into account. Diffusion effects can be inserted but require great precaution. However, it gives access to the medium frequency range mentioned above. Specular reflection – originating from geometrical optics concepts – applied to sound waves in air is quoted as early as the 1940s [1] if not before, with experimental validation. The principle of specular reflection on perfectly rigid walls is compatible with the modal theory in waveguides and in rectangular cavities [2]. It is also with specular reflection that it has been possible to obtain an understanding of some causality problems in the field of active acoustic control [3], as long as the geometrical configuration is very simple. In architectural acoustics, it is commonly accepted that the ray method is able to describe sound fields above 100Hz in large auditoriums [4]. Here, the calculation of the field at some particular point within the domain does not require that of the entire domain (contrarily to the finite element method) nor on all the boundaries (contrarily to the boundary element method). However, one has to remember that the method is not rigorous and that the reaction taken only at the impact point of reflection is an approximation of the more global reaction properly described by the integral representation; this is probably the reason why calculation on all the boundaries is not needed.

The ray method, so widely known for room acoustics in the years around 1960/90 [5], has been revisited over the last ten years or so for its use in vehicle passengers' space, with the sound field descriptions in the audible medium frequency range in view [6, 7]. Concerning the algorithmic procedure, improvements carried out by previous authors in two different directions are helpful [4, 8, 9]: one is called *ray-tracing*, the other *virtual image sources*, and their history shows that they were developed quite simultaneously.

In a *ray-tracing* algorithm, rays "leave" a point source emitting an impulse (in theory an infinity of rays) and, for each of them, the first point of impact on a wall is sought and from there on the next impact point on another wall, etc … Nothing prevents this method from being used within non convex cavities. A priori, the procedure goes on indefinitely for each ray. Given a receiver point R, rays originating from the source that, after a certain number of reflections, go through R, make up the sound history – called impulse response or histogram or echogram – at point R. In practice, the number of rays leaving the source is finite and the rays propagate in a divergent way with the consequence that the weaker the probability for the rays to go through the receiver R, the smaller the number of permitted reflections. This is the reason why the histogram is made for a neighbourhood of R rather than the point alone. In these conditions the procedure can be quite short but at the price of uncertainty. Nevertheless, this ray-tracing version has the great advantage of being able to insert diffusive walls (because of their geometry and not of their behaviour).

The *virtual image sources* algorithm identifies the images of the real source by a mirror effect on each wall, then the images of the images are sought, etc …, a priori indefinitely. However all these images are only potentially useful for calculating the acoustic field (except for rectangular enclosures) and only a small number of them actually "light" the domain, while still less are "seen" by the given receiver point. Validity (for "lighting" the domain) and visibility (of the receiver point) tests reduce hugely the number of images and a proximity test restricts their number by limiting the acceptable distance between the images and the receiver point. Non-convex domains need an obstruction test [9] or call for another approach [7, 10]. The algorithm is precise in giving the rays leaving the source and propagating to the receiver, but distinguishing the useful sources from the potential ones is a heavy task and moreover it is difficult here to take

diffusion into account. However, this procedure is chosen in this paper for its precision. It has to be mentioned that the virtual sources procedure can also be understood as that of virtual receivers. Indeed, by determining the receiver images it is possible to retro-propagate rays issued from R until the real source is reached [9]. At this stage, it must be noted that the definition of image sources makes the problem independent of the type of signal emitted by the primary source and of the usage of the signal at the reception point. For example, in [4, 8, 9], rays are energy carriers and are used to assess sound intensity (under consideration of the form of the sound field). Here, phased (therefore in terms of complex amplitudes) sound fields in the frequency domain are considered, so as to observe systems of standing waves forming resonances and anti-resonances.

In that sense, comparison between acoustic fields calculated by the finite element method and the ray method (with the image source algorithm) has shown differences which constitute a handicap for going further in small enclosures with the latter method [7]. What ought then to be done in order to reduce the differences? It is known qualitatively that the ray method does not take into account diffraction and/or diffusion and that the solution obtained cannot in general be exact. But even by dealing only with the part of the acoustic field made up of specular reflections, what do we know quantitatively about the ability of the image sources to reveal the field? In trying to answer this question, it would first be necessary to sustain the intuitive notion of image sources by a rational formulation and, in doing so, to have a tool to master their contribution to the sound field. Looking in that direction in the framework of a very elementary geometrical configuration, it has been found that sources said to be invalid by the current source-choosing algorithm could improve the description of the acoustic field. This being said, it has not yet been possible to know if this improvement resulted from a better description of diffraction, or

of the reflected field, or of both. Thus, the work presented here has the form of a theoretical investigation in a simple configuration, an investigation not yet found in the acoustic literature.

The beginning of this paper is a recall of one of the algorithms of the ray method that defines the image sources, and also emphasizes two figures of an angular sector in the plane which motivate the study. After a first premiss that sets out a particular presentation of the acoustic field in presence of a reflective wall in a 2D half-space, the exact solution of the angular sector arises from the integral representation. The solution thus obtained on the walls is liable to be developed in series, and arguments associated with the Huygens' Principle lead us to think that each term of the series could reveal the contribution of an image source. The same formalism is then extended to the case of walls with damping material. Then, the transformation of the pressure on the walls into the pressure inside the sector shows the possible contribution of image sources inside the domain. Numerical experiments in the third section of this paper support broadly the hypothesis of a correspondence between terms of the series and image source contributions, opening a door towards an improvement of the current algorithms for identifying the useful virtual sources.

At this point it is necessary to cite in more detail the work of Mechel [10], presenting a comprehensive overview of the image sources method. The reassembling of sources in a 2D angular sector and the development of the exact solution into a modal series (different from the series development presented in this paper) are of particular interest here. The reassembling of sources leads to the definition and the insertion of a "corner source", along with a particular directivity, and to an algorithm to compute the validity of images. The modal series suggests the idea of inserting the exact solution into the image sources method, thereby resulting in a mixed analytical-image source method. Although the approach presented here has not been inspired by

Mechel's work and follows a different path, a certain relation between the objectives of both approaches must be assessed. In fact, these two approaches could converge by extrapolation of the fact that the elementary solution classically associated with each image source could be replaced by a more complete solution (including diffraction) associated with a certain set of images.

The present text develops, extends and explores in greater depth the subject of a relatively short communication given recently at a congress [11].

II – FORMALISM ON THE BOUNDARIES AND IN THE DOMAIN

A. Preamble, configurations and premisses

Any comparison between acoustic fields obtained by the image source method and by the boundary integral method needs, as a preliminary, to speak of the algorithm which usually chooses the image sources. The image from a wall numbered n originates by a mirror effect on that wall from a source, that could itself be the image from wall numbered k. It is convenient to write it as $S_{\underbrace{.....kn}_{l \text{ indices}}}$ to signify that it will give rise to l reflections from the actual source, the last one on wall n, the previous one on wall k, etc... For example, the source denoted S_5 is the image of the real source through wall 5, and source S_{53} is the image of source S_5 through wall 3. Its presence will show two reflections. This can happen only if the last reflection is able to reach a point inside the domain. To clarify, Figure 1 presents a 2D domain made up of an angular sector defined by two semi-infinite straight lines, in fact two segments (of finite length). Six image sources are liable to reveal reflections. However to reach point P, only four image-sources

are useful; only source S_{212} would give a reflected ray reaching point Q ; for R , three image sources intervene. In Figure 1, it appears that an image source with last index n plays a role, for point P for instance, if the ray from that source goes through wall n to reach P . In these conditions, source S_{212} is of no use for point Q as the ray from S_{212} does not go through wall Γ_2 to reach Q .

Having thus in mind the algorithm for determining the sources, the motivation of the present work arises from both diagrams in Figure 2. The sector is now defined by the semi-infinite straight lines Γ_1 and Γ_2 . The configuration on the left leads to four sources (three images and the real source). However, the validity of the field obtained at point Q_1 is not guaranteed. On the contrary, to the right, the only image source available definitively instills a doubt regarding the field obtained, as it is not expected that wall Γ_2 plays no role at all (source S_1 reveals the presence of wall Γ_1 only). Nevertheless, it is possible to enlighten the degree of precision of the field obtained by rays by comparing it to the exact solution given by the integral representation. To begin with, the particularly simple situation of a single reflecting plane is observed to gain access to the definition of the first order image source, the wall pressure (in a discretized form) and an iterative access to it. Notations will be defined in the course of development. In Figure 3, a point source S_0 radiates an acoustic pressure. In particular at point Q on the perfectly reflecting wall Γ , the elementary solution of the Helmholtz operator is shown to be

$$p(Q) = G_\infty(Q,S_0) + G_\infty(Q,S_0) \qquad (1)$$

where $G_\infty(Q,S_0)$ is the elementary solution of the Helmholtz operator in an open domain (the source flow amplitude is chosen so that the right hand side of the Helmholtz wave equation is

unity); here, in 2D, it has the form $-\frac{i}{4} H_0^-(k|Q-S_0|)$ with H_0^- the Hankel function of the 2nd kind of 0th order. In fact, for any point R in the domain, the integral representation (also called Green's third formula) leads to

$$p(R) = G_\infty(R,S_0) + \int_\Gamma \partial_{n_M} G_\infty(R,M)\, p(M)\, dM \qquad (2)$$

where $G_\infty(R,S_0)$ is the result of the operation $\int_\Omega G_\infty(R,S)\, \delta(S - S_0)\, dS$ taking into account the excitation on the right hand side of the wave equation.

When point R in the domain tends toward point Q on Γ, the principal part of the double layer potential leads to

$$p(Q) = G_\infty(Q,S_0) + \frac{1}{2} p(Q) \qquad (3)$$

which can also be written

$$p(Q) = 2G_\infty(Q,S_0) \;\forall Q \in \Gamma \qquad (4)$$

and $p(\Gamma) = 2G_0(\Gamma)$ will now be a shorthand representation for $p(Q) = 2G_\infty(Q,S_0)$ when the observation points Q are on the boundary Γ. The subscript 0 is linked to the source S_0 (the index ∞ of G has been removed when indication of the source occurs). The image source S_1 can be made apparent by noting

$$p(\Gamma) = \underbrace{G_0(\Gamma)}_{\text{coming from } S_0} + \underbrace{\frac{1}{2} p(\Gamma)}_{\text{coming from } S_1} \qquad (5)$$

In fact, the term $\frac{1}{2} p(\Gamma)$ in (5) is equal to $G_\infty(Q,S_0)$ by identification in (3) and (4). It indeed represents the free-field pressure on the geometrical locus Γ due to S_0 but also the pressure on

the same locus due to S_1, since S_1 is the mirror image of S_0 relative to Γ.

Now, out of the continuous form

$$p(Q) = G_\infty(Q,S_0) + \int_\Gamma p(M)\, \partial_{n_M} G_\infty(Q,M)\, dM \qquad (6)$$

a discrete form can be deduced. By decomposing the wall Γ (which is a straight line in this bi-dimensional space) into elementary facets Γ_j such as $\Gamma \equiv \cup\Gamma_j$ with $j = 1,\infty$, equation (6) can be approximated by

$$p(Q) = G_\infty(Q,S_0) + \sum_{j=1}^{\infty} p(M_j) \int_{\Gamma_j} \partial_{n_M} G_\infty(Q,M)\, dM \quad \text{where} \quad M_j \in \Gamma_j \qquad (7)$$

provided the pressure can be considered constant on each facet. For a particular point Q_i, the pressure can be written

$$p_i = G_\infty(Q_i,S_0) + \sum_{j=1}^{\infty} a_{ij} p_j \qquad (8)$$

or, for a set of points on the wall, by the matrix equation

$$\mathbf{p}(\Gamma) = \mathbf{g}_0(\Gamma) + \mathbf{A}.\mathbf{p}(\Gamma) \qquad (9)$$

where the vertical (columns) dimension of matrix **A** is infinite. Following the usual convention, bold lowercase letters represent vectors and bold uppercase ones represent matrices ; accordingly $G_\infty(Q_i,S_0)$ becomes $\mathbf{g}_0(\Gamma)$. For the resolution of the problem, **A** will be made square and (3) provides that

$$\mathbf{A} = \frac{1}{2}\mathbf{I} \qquad (10)$$

in that case.

At this stage, a side remark will be useful for the later developments. In (9), the wall pressure $\mathbf{p}(\Gamma)$ is the final solution sought, which will be written $\mathbf{p}_E$ (E for “end”). The term

$\mathbf{g}_0(\Gamma)$ comes from the free-field pressure on the geometrical locus on the wall and will be thus written $\mathbf{p}_F$ (F for "free"). In these conditions, (9) becomes

$$\mathbf{p}_E = [\mathbf{I}- \mathbf{A}]^{-1}.\mathbf{p}_F \qquad (11)$$

which describes the effect of the wall on the free-field emitted by the source S_0. This formulation can also be differently interpreted if one considers equation (11) with the matrix term formally developed as a series:

$$\mathbf{p}_E = \underbrace{\mathbf{p}_F}_{\text{contribution from } S_0} + \underbrace{[\mathbf{A}+\mathbf{A}^2+\mathbf{A}^3+...].\mathbf{p}_F}_{\text{contribution from } S_1 \text{ taking the wall into account}} \qquad (12)$$

In fact, with no absorption where (10) is valid, the second term of the right hand side of (12) leads to

$$(\frac{1}{2}+\frac{1}{4}+\frac{1}{8}+...)\,\mathbf{p}_F = \mathbf{p}_F \qquad (13)$$

which is the contribution of the image source S_1. The existence of this source takes the wall into account and its contribution with $\mathbf{p}_F = 1/2\,\mathbf{p}_E$ reveals that the wall reflects perfectly.

Furthermore, if $\mathbf{A}$ is seen as revealing the radiation of a pressure source upon itself, the modified pressure value becomes the new pressure source, which is again modified by $\mathbf{A}$ etc…, and the pressure at the source converges towards the pressure value $1/2\,\mathbf{p}_E = \mathbf{p}_F$ in vector notation. This interpretation would then be a special case of what will be discussed later on. It should also be noted that the development of $[\mathbf{I}- \mathbf{A}]^{-1}$ is legitimate as long as the series converges. It is evidently the case here, but in a more general case, the convergence of the series should be assessed.

B. A possible origin of the image sources and of their relative importance

Were the ray method exact, the pressure on point Q_1 on wall Γ_1 in Figure 2(a) would be, with the notations mentioned before

$$p_{ray}(Q_1) = G_0(Q_1) + G_1(Q_1) + G_2(Q_1) + G_{21}(Q_1) \tag{14}$$

As previously stated, (14) is more precisely written in 2D as

$$p_{ray}(Q_1) = -\frac{i}{4}\left(H_0^-(k|Q_1 - S_0|) + H_0^-(k|Q_1 - S_1|) + H_0^-(k|Q_1 - S_2|) + H_0^-(k|Q_1 - S_{21}|)\right) \tag{15}$$

What would be the outcome of a computation from integral representation, which is known to be exact? To start with, the development is done with non-absorbing walls.

Green's third formula leads to

$$p(Q_1) = G_\infty(S_0,Q_1) + \underbrace{\int_{\Gamma_1} p(M)\,\partial_{n_M} G_\infty(Q_1,M)\,dM}_{=1/2\,p(Q_1)} + \int_{\Gamma_2} p(M)\,\partial_{n_M} G_\infty(Q_1,M)\,dM \tag{16}$$

or, in matrix form, with still further obvious shorthand representation

$$\mathbf{p}(\Gamma_1) = \mathbf{p}_1 = \mathbf{g}_0(\Gamma_1) + \mathbf{A}_{11}.\mathbf{p}_1 + \mathbf{A}_{12}.\mathbf{p}_2 \tag{17}$$

with

$$\mathbf{A}_{11} = \frac{1}{2}\,\mathbf{I} \tag{18}$$

in the case of a perfectly reflecting wall Γ_1. In a similar way,

$$\mathbf{p}_2 = \mathbf{g}_0(\Gamma_2) + \mathbf{A}_{21}.\mathbf{p}_1 + \mathbf{A}_{22}.\mathbf{p}_2 \tag{19}$$

with

$$\mathbf{A}_{22} = \frac{1}{2}\,\mathbf{I} \tag{20}$$

with a perfectly reflecting wall Γ_2. It is to be noted that (18) and (20) reveal infinite and perfectly reflecting walls. The matrices $\mathbf{A}_{12}$ and $\mathbf{A}_{21}$ therefore contain information about the finiteness of the walls (they are of semi-infinite dimensions) and border effects.

Equations (17) and (19) lead to

$$\begin{aligned}
\mathbf{p}_1 = & \underbrace{\underbrace{[\mathbf{I} - \mathbf{A}_{11}]^{-1}}_{=2\,\mathbf{I} \text{ when } \beta=0} \cdot \mathbf{g}_0(\Gamma_1)}_{\substack{\text{contributions of } S_0 \text{ and } S_1 \text{ on } \Gamma_1 \\ \text{respectively noted } \mathbf{g}_0(\Gamma_1) \text{ and } \mathbf{g}_1(\Gamma_1)}} + \underbrace{[\mathbf{I} - \mathbf{A}_{11}]^{-1} \cdot \mathbf{A}_{12}}_{=2\,\mathbf{A}_{12} \text{ noted } 2\,\mathbf{C}} \cdot \mathbf{p}_2 \\
\mathbf{p}_2 = & \underbrace{[\mathbf{I} - \mathbf{A}_{22}]^{-1} \cdot \mathbf{g}_0(\Gamma_2)}_{\substack{\text{contributions of } S_0 \text{ and } S_2 \text{ on } \Gamma_2 \\ \text{respectively noted } \mathbf{g}_0(\Gamma_2) \text{ and } \mathbf{g}_2(\Gamma_2)}} + \underbrace{[\mathbf{I} - \mathbf{A}_{22}]^{-1} \cdot \mathbf{A}_{21}}_{=2\,\mathbf{A}_{21} \text{ noted } 2\,\mathbf{B}} \cdot \mathbf{p}_1
\end{aligned} \tag{21}$$

where equation (10) with reflecting walls (admittance $\beta=0$) has been used and where matrices $\mathbf{B}$ and $\mathbf{C}$ are a notation used for brevity's sake. Solving this system provides

$$\begin{aligned}
\mathbf{p_1} &= [\mathbf{I} - 2\mathbf{C} \cdot 2\mathbf{B}]^{-1} \cdot \left(\mathbf{g_0}(\Gamma_1) + \mathbf{g_1}(\Gamma_1)\right) + [\mathbf{I} - 2\mathbf{C} \cdot 2\mathbf{B}]^{-1} \cdot 2\mathbf{C} \cdot \left(\mathbf{g_0}(\Gamma_2) + \mathbf{g_2}(\Gamma_2)\right) \\
\mathbf{p_2} &= [\mathbf{I} - 2\mathbf{B} \cdot 2\mathbf{C}]^{-1} \cdot \left(\mathbf{g_0}(\Gamma_2) + \mathbf{g_2}(\Gamma_2)\right) + [\mathbf{I} - 2\mathbf{B} \cdot 2\mathbf{C}]^{-1} \cdot 2\mathbf{B} \cdot \left(\mathbf{g_0}(\Gamma_1) + \mathbf{g_1}(\Gamma_1)\right)
\end{aligned} \tag{22}$$

Formally, developing in series would result in the expressions

$$\begin{aligned}
\mathbf{p_1} = & \mathbf{g_0}(\Gamma_1) + \mathbf{g_1}(\Gamma_1) + 2\mathbf{C} \cdot \left(\mathbf{g_0}(\Gamma_2) + \mathbf{g_2}(\Gamma_2)\right) \\
& + 2\mathbf{C} \cdot 2\mathbf{B} \cdot \left(\mathbf{g_0}(\Gamma_1) + \mathbf{g_1}(\Gamma_1)\right) + 2\mathbf{C} \cdot 2\mathbf{B} \cdot 2\mathbf{C} \cdot \left(\mathbf{g_0}(\Gamma_2) + \mathbf{g_2}(\Gamma_2)\right) + \ldots \\
\mathbf{p}_2 = & \mathbf{g_0}(\Gamma_2) + \mathbf{g_2}(\Gamma_2) + 2\mathbf{B} \cdot \left(\mathbf{g_0}(\Gamma_1) + \mathbf{g_1}(\Gamma_1)\right) \\
& + 2\mathbf{B} \cdot 2\mathbf{C} \cdot \left(\mathbf{g_0}(\Gamma_2) + \mathbf{g_2}(\Gamma_2)\right) + 2\mathbf{B} \cdot 2\mathbf{C} \cdot 2\mathbf{B} \cdot \left(\mathbf{g_0}(\Gamma_1) + \mathbf{g_1}(\Gamma_1)\right) + \ldots
\end{aligned} \tag{23}$$

Now, Huygens' Principle posits that the field emitted from a source to a reception point can be regarded as the contribution of fictitious sources located on the wavefront between the source and the reception point [12]. This assertion, qualitative at this stage, argues in favour of establishing a correlation between the terms of the series and the image sources. Indeed, keeping an eye on $\mathbf{p_1}$ in (23), it should be noted that $2\mathbf{C} \cdot \mathbf{g_0}(\Gamma_2)$ is the pressure radiated by S_0 toward Γ_2

transferred to Γ_1 through the multiplication by $2\mathbf{C}$ (cf. Figure 4). It is also the pressure originating from S_2 on Γ_2 transferred to Γ_1, i.e. pressure from S_2 radiated to Γ_1 denoted $\mathbf{g_2}(\Gamma_1)$. This last deduction lacks rigour for the time being. In fact, it would be necessary to know the pressure radiated by S_2 on the whole (infinite) wall Γ_2 for the pressure transferred to points of Γ_1 to be comparable with that radiated by S_2. To this first reasoning, another is added. Term $2\mathbf{C}\cdot\mathbf{g_2}(\Gamma_2)$ represents the pressure due to S_2 on Γ_2 transferred to Γ_1 i.e. pressure from S_2 on Γ_1. It is also the pressure from S_{21} to Γ_1 or $\mathbf{g_{21}}(\Gamma_1)$, with the same lack of rigour as written above (the notation $\mathbf{g_{21}}$ for source S_{21} is clear, see section II-1 for the definition of S_{21}). With both reasonings, it appears from (23) (terms of the same order are in brackets)

$$\begin{aligned}\mathbf{p_1} &= \left[\mathbf{g_0}(\Gamma_1)+\mathbf{g_1}(\Gamma_1)\right]+\left[\mathbf{g_2}(\Gamma_1)+\mathbf{g_{21}}(\Gamma_1)\right]+\left[\mathbf{g_{12}}(\Gamma_1)+\mathbf{g_{121}}(\Gamma_1)\right]+\left[\mathbf{g_{212}}(\Gamma_1)+\mathbf{g_{2121}}(\Gamma_1)\right]+\ldots\\ \mathbf{p_2} &= \underbrace{\left[\mathbf{g_0}(\Gamma_2)+\mathbf{g_2}(\Gamma_2)\right]}_{0^{\text{th}}\text{ order terms}}+\underbrace{\left[\mathbf{g_1}(\Gamma_2)+\mathbf{g_{12}}(\Gamma_2)\right]}_{1^{\text{st}}\text{ order terms}}+\underbrace{\left[\mathbf{g_{21}}(\Gamma_2)+\mathbf{g_{212}}(\Gamma_2)\right]}_{2^{\text{nd}}\text{ order terms}}+\underbrace{\left[\mathbf{g_{121}}(\Gamma_2)+\mathbf{g_{1212}}(\Gamma_2)\right]}_{3^{\text{rd}}\text{ order terms}}+\ldots\end{aligned} \quad (24)$$

To put the above formalism in relation with the diagrams of motivation in Figure 2, we ought to conclude that the sources S_{12}, S_{121}, etc… are missing on the left configuration (see Figure 2a), and sources S_2, S_{21}, etc… for the configuration on the right (Figure 2b). Moreover, taking into account the natural order of terms in the series for $\mathbf{p_1}$, the first source that ought to be added to the configuration on the left would be S_{12}, which is not suitable since it is inside the domain. On the right configuration, source S_2 ought to be considered next. The algorithm for determining the sources would take it into account, were wall 2 lengthened towards the left. Let us also note that the order of sources for $\mathbf{p_1}$ is not the same as for $\mathbf{p_2}$.

Studying the same problem with an admittance β_1 on Γ_1 and β_2 on Γ_2 enables us on the one hand, to refine the transfer terms towards walls Γ_1 and Γ_2 and, on the other hand, to take the

admittance of the reflections associated with the image sources into account. The development resembles the one presented at the start of this section, but with a further degree of generalization along with some refinements in the possible understanding of the image sources origin.

In this case also, some preliminary remarks are necessary and one returns to Figure 3, where the wall Γ now has an admittance β_Γ (the inverse of the reduced impedance Z_Γ). Equation (6) is now to be written

$$p(R) = G_\infty(R,S_0) + \int_\Gamma \underbrace{\left(\partial_{n_M} G_\infty(R,M) + ik\beta_\Gamma\ G_\infty(R,M)\right)}_{(*)}\ p(M)\ dM \qquad (25)$$

So the wall itself takes on the role of a source with pressure $p(M)$, transmitted to point R while considering the wall admittance β_Γ and the radiation via $\partial_{n_M} G_\infty$ and G_∞ applied to the distance $|R\text{-}M|$. From a physical viewpoint, the so-called source pressure $p(M)$ must act on the internal source impedance Z_Γ combined with the load impedance coming from the medium in which the acoustical pressure is propagating. The resulting pressure must then be propagated to point R. All these roles are described by part (*) of equation (25). In terms of discrete operators, making point R tend toward point Q on wall Γ leads to

$$p(Q) - \int_\Gamma \left(\partial_{n_M} G_\infty(Q,M) + ik\beta_\Gamma\ G_\infty(Q,M)\right)\ p(M)\ dM = G_\infty(Q,S_0) \qquad (26)$$

or, by using the same notations as in (11)

$$\mathbf{p}_E(\Gamma) = [\mathbf{I} - \mathbf{A}_{\Gamma\Gamma}]^{-1} \cdot \mathbf{p}_F(\Gamma) \qquad (27)$$

where the matrix $\mathbf{A}_{\Gamma\Gamma}$ (a generalization of the form $\mathbf{A}$ in (11), representing the influence of the wall facets on observation points on the wall) stems from a discretized form of the expression

$$\int_\Gamma \left(\partial_{n_M} G_\infty(Q,M) + ik\beta_\Gamma\ G_\infty(Q,M)\right)\ p(M)\ dM \qquad (28)$$

In the whole domain, with $\mathbf{p}_E(\Omega)$ noting the vector containing pressure values on points inside the domain and with $\mathbf{A}_{\Omega\Gamma}$ noting the matrix originating from the discretization of

$$\int_\Gamma \left(\partial_{n_M} G_\infty(R,M) + ik\beta_\Gamma\ G_\infty(R,M)\right) p(M)\, dM \qquad (29)$$

the components of which represent the influence on the facets on the reception point in the domain, equation (25) becomes

$$\mathbf{p}_E(\Omega) = \mathbf{A}_{\Omega\Gamma} \cdot [\mathbf{I} - \mathbf{A}_{\Gamma\Gamma}]^{-1} \cdot \mathbf{p}_F(\Gamma) + \mathbf{g}_0(\Omega) \qquad (30)$$

This can be interpreted as follows: $\mathbf{p}_F(\Gamma)$ is the pressure coming from source S_0 radiated on the geometrical locus defined by the wall Γ, S_0 loaded by both its internal impedance Z_{S_0} and the radiating impedance Z_{rad_Ω}. This pressure is therefore more precisely written

$$\mathbf{p}_F(\Gamma) = \mathbf{g}_0(Z_{S_0} \cup Z_{rad_\Omega}, \Gamma^{geom}) \qquad (31)$$

The operator $[\mathbf{I} - \mathbf{A}_{\Gamma\Gamma}]^{-1}$ applied to this quantity does consider the wall impedance (in fact the combination of the wall and propagation medium impedances) and one writes

$$\mathbf{p}_E(\Gamma) = [\mathbf{I} - \mathbf{A}_{\Gamma\Gamma}]^{-1} \cdot \mathbf{p}_F(\Gamma) = \underbrace{\mathbf{g}_0(Z_{S_0} \cup Z_{rad_\Omega}, \Gamma(Z_\Gamma))}_{\mathbf{g}_1(Z_{S_0} \cup Z_{rad_\Omega}, \Gamma(Z_\Gamma))} \qquad (32)$$

where it has been emphasized that Γ is now no longer only a geometrical locus but also an actual wall with some kind of internal impedance if this wall is to be seen as a source. Furthermore, as for equation (5), it appears that the pressure emitted by S_0 on the wall is also the pressure emitted by image S_1.

Finally, the right side of equation (30), except the direct contribution, is interpreted as the pressure coming from the image source on a geometrical locus of the domain and will be written

$$\mathbf{A}_{\Omega\Gamma} \cdot [\mathbf{I} - \mathbf{A}_{\Gamma\Gamma}]^{-1} \cdot \mathbf{p}_F(\Gamma) = \mathbf{g}_1(Z_{S_0} \cup Z_{rad_\Omega}, Z_\Gamma \cup Z_{rad_\Gamma}, \Omega^{geom}) \qquad (33)$$

This rich notation reveals that the image source S_1 emits a pressure towards a point inside the domain Ω, taking into account the fact that it is the image of source S_0 (together with its internal impedance Z_{S_0} and load Z_{rad_Ω}) relatively to wall Γ (with internal impedance Z_Γ and load Z_{rad_Γ}).

The notion of a wall seen as a source with its own pressure and having an internal impedance that must be combined with the load impedance in order to radiate into the domain – or toward the geometrical locus of another wall – is the key to interpreting the terms of the series development of the solution obtained by the integral equations method.

Going back to the situations in Figure 2, the continuous form of the coupled problem on both walls is now the extended form of (16)

$$\begin{cases} p(Q_1) = G_\infty(Q_1,S_0) + \int_{\Gamma_1} p(M)\left(\partial_{n_M} G_\infty(Q_1,M) + ik\,\beta_1\, G_\infty(Q_1,M)\right)dM \\ \qquad\qquad + \int_{\Gamma_2} p(M)\left(\partial_{n_M} G_\infty(Q_1,M) + ik\,\beta_2\, G_\infty(Q_1,M)\right)dM \\ p(Q_2) = G_\infty(Q_2,S_0) + \int_{\Gamma_1} p(M)\left(\partial_{n_M} G_\infty(Q_2,M) + ik\,\beta_1\, G_\infty(Q_2,M)\right)dM \\ \qquad\qquad + \int_{\Gamma_2} p(M)\left(\partial_{n_M} G_\infty(Q_2,M) + ik\,\beta_2\, G_\infty(Q_2,M)\right)dM \end{cases} \tag{34}$$

or in discrete form (this time, unlike (21), without simplification)

$$\begin{cases} \mathbf{p}_1 = [\mathbf{I} - \mathbf{A}_{11}]^{-1} \cdot \mathbf{g}_0(\Gamma_1) + [\mathbf{I} - \mathbf{A}_{11}]^{-1} \cdot \mathbf{A}_{12} \cdot \mathbf{p}_2 \\ \mathbf{p}_2 = [\mathbf{I} - \mathbf{A}_{22}]^{-1} \cdot \mathbf{g}_0(\Gamma_2) + [\mathbf{I} - \mathbf{A}_{22}]^{-1} \cdot \mathbf{A}_{21} \cdot \mathbf{p}_1 \end{cases} \tag{35}$$

out of which one obtains for example the extended form of (22)

$$\begin{aligned} \mathbf{p}_1 = &\left[\mathbf{I} - [\mathbf{I} - \mathbf{A}_{11}]^{-1} \cdot \mathbf{A}_{12} \cdot [\mathbf{I} - \mathbf{A}_{22}]^{-1} \cdot \mathbf{A}_{21}\right]^{-1} \\ &\cdot \left[[\mathbf{I} - \mathbf{A}_{11}]^{-1} \cdot \mathbf{g}_0(\Gamma_1) + [\mathbf{I} - \mathbf{A}_{11}]^{-1} \cdot \mathbf{A}_{12} \cdot [\mathbf{I} - \mathbf{A}_{22}]^{-1} \cdot \mathbf{g}_0(\Gamma_2)\right] \end{aligned} \tag{36}$$

Using the notations $\mathbf{D}_{21} = [\mathbf{I} - \mathbf{A}_{22}]^{-1} \cdot \mathbf{A}_{21}$ and $\mathbf{D}_{12} = [\mathbf{I} - \mathbf{A}_{11}]^{-1} \cdot \mathbf{A}_{12}$ the terms responsible for the pressure transfer from Γ_1 to Γ_2 and inversely appear; they generalize matrices 2**B** and 2**C** in (21). The order of the indices comes from the matrix equations and must be read from right to left to reveal the direction of transfer from one wall to the other. The analysis of $\mathbf{D}_{21}$, for example, shows that $\mathbf{A}_{21}$, which originates from

$$\int_{\Gamma_1} \left(\partial_{n_M} G_\infty(Q_2,M) + ik\,\beta_1\, G_\infty(Q_2,M) \right) p(M)\, dM \qquad (37)$$

applied to $p(\Gamma_1)$ makes wall Γ_1 (with pressure $p(\Gamma_1)$ and internal impedance Z_1) radiate towards the locus defined by wall Γ_2. Moreover, according to equation (27), the operator $[\mathbf{I} - \mathbf{A}_{22}]^{-1}$ modifies the pressure radiated at Γ_2 so as to consider the absorption described by β_2. Figure 5 illustrates the action of the operators $\mathbf{D}_{21}$ and $\mathbf{D}_{12}$. At this stage, the pressure at equation (36) is now

$$\mathbf{p}_1 = \left[\mathbf{I} - \mathbf{D}_{12} \cdot \mathbf{D}_{21}\right]^{-1} \cdot \left[[\mathbf{I} - \mathbf{A}_{11}]^{-1} \cdot \mathbf{g}_0(\Gamma_1) + \mathbf{D}_{12} \cdot [\mathbf{I} - \mathbf{A}_{22}]^{-1} \cdot \mathbf{g}_0(\Gamma_2) \right] \qquad (38)$$

and, using Eq. (12) as well as the remarks in Eq. (21), it can be written

$$\mathbf{p}_1 = \left[\mathbf{I} - \mathbf{D}_{12} \cdot \mathbf{D}_{21}\right]^{-1} \cdot \left[\left(\mathbf{g}_0(\Gamma_1) + \mathbf{g}_1(\Gamma_1, \beta_1) \right) + \mathbf{D}_{12} \cdot \left(\mathbf{g}_0(\Gamma_2) + \mathbf{g}_2(\Gamma_2, \beta_2) \right) \right] \qquad (39)$$

where the expression $\mathbf{g}_1(\Gamma_1, \beta_1)$ stipulates that S_1 radiates on Γ_1, taking the wall admittance β_1 into account, and similarly for $\mathbf{g}_2(\Gamma_2, \beta_2)$. By developing the inverse term in (35) we obtain

$$\begin{aligned} \mathbf{p}_1 = & \left(\mathbf{g}_0(\Gamma_1) + \mathbf{g}_1(\Gamma_1, \beta_1) \right) + \mathbf{D}_{12} \cdot \left(\mathbf{g}_0(\Gamma_2) + \mathbf{g}_2(\Gamma_2, \beta_2) \right) \\ & + \mathbf{D}_{12} \cdot \mathbf{D}_{21} \cdot \left(\mathbf{g}_0(\Gamma_1) + \mathbf{g}_1(\Gamma_1, \beta_1) \right) + \mathbf{D}_{12} \cdot \mathbf{D}_{21} \cdot \mathbf{D}_{12} \cdot \left(\mathbf{g}_0(\Gamma_2) + \mathbf{g}_2(\Gamma_2, \beta_2) \right) + \ldots \end{aligned} \qquad (40)$$

which is a generalization of (23).

The terms in equation (40) should be analysed as follows. The symbol $\mathbf{g}_0(\Gamma_1)$ is the pressure radiated at geometrical locus Γ_1 coming from source S_0 (with its own pressure and impedance). The radiation uses a combination of source and radiation impedances and one notes more precisely as in (31)

$$\mathbf{g}_0(\Gamma_1) = \mathbf{g}_0(Z_{S_0} \cup Z_{rad_\Omega}, \Gamma_1^{geom}) \tag{41}$$

and accordingly

$$\mathbf{g}_0(\Gamma_2) = \mathbf{g}_0(Z_{S_0} \cup Z_{rad_\Omega}, \Gamma_2^{geom}) \tag{42}$$

Similarly to the case with reflecting walls, it is supposed that the term $\mathbf{D}_{12}.\mathbf{g}_0(\Gamma_2)$ is at the origin of term $\mathbf{g}_2(\Gamma_1)$, but now for absorbing walls a more precise interpretation is sought. With the notations introduced before, this term is

$$\mathbf{D}_{12}.\mathbf{g}_0(\Gamma_2) = [\mathbf{I} - \mathbf{A}_{11}]^{-1}.\ \mathbf{A}_{12}.\ \mathbf{g}_0(\Gamma_2) \tag{43}$$

The operator $\mathbf{A}_{12}$ applied to $\mathbf{g}_0(\Gamma_2)$ (the precise form of which is written as (42)) arises from the continuous term

$$\int_{\Gamma_2} \underbrace{\left(\partial_{n_M} G_\infty(Q_1,M) + ik\,\beta_2\ G_\infty(Q_1,M)\right)}_{(*)}\ G_0(Z_{S_0} \cup Z_{rad_\Omega}, \Gamma_2^{geom}(M))\ dM \tag{44}$$

(G_0 is the Green function corresponding to vector $\mathbf{g}_0$) where some conjectures had to be accepted in order to go further in the interpretation. In equation (44), the term $G_0(Z_{S_0} \cup Z_{rad_\Omega}, \Gamma_2^{geom}(M))$ could have the role of the pressure coming from Γ_2 seen as a source radiating toward geometrical locus Γ_1^{geom}. To this end, it should have a source impedance and a radiation impedance. This source would then be revealed by the existence of the image source S_2. The term (*) in equation (44) could have this role of combining both source and radiation impedances. In these conditions,

$$\mathbf{A}_{12} \cdot \mathbf{g}_0(Z_{S_0} \cup Z_{\mathrm{rad}_\Omega}, \Gamma_2^{\mathrm{geom}}) \equiv \mathbf{g}_2\left(Z_{S_0} \cup Z_{\mathrm{rad}_\Omega}, Z_2 \cup Z_{\mathrm{rad}_{\Gamma_2}}, \Gamma_1^{\mathrm{geom}}\right) \qquad (45)$$

and, following the interpretation of (37),

$$\mathbf{D}_{12} \cdot \mathbf{g}_0(\Gamma_2) = [\mathbf{I} - \mathbf{A}_{11}]^{-1} \cdot \mathbf{A}_{12} \cdot \mathbf{g}_0(Z_{S_0} \cup Z_{\mathrm{rad}_\Omega}, \Gamma_2^{\mathrm{geom}}) \equiv \mathbf{g}_2\left((Z_{S_0} \cup Z_{\mathrm{rad}_\Omega}), (Z_2 \cup Z_{\mathrm{rad}_{\Gamma_2}}), \Gamma_1(Z_1)\right) \quad (46)$$

thus confirming the first supposition. Encouraged by this understanding of the term $\mathbf{D}_{12} \cdot \mathbf{g}_0(\Gamma_2)$, a similar interpretation of term $\mathbf{D}_{21} \cdot \mathbf{D}_{12} \cdot \mathbf{g}_0(\Gamma_2)$ is sought. It is expected that expression (46) allows for

$$\mathbf{D}_{21} \cdot \mathbf{D}_{12} \cdot \mathbf{g}_0(\Gamma_2) \equiv \mathbf{g}_{21}\left(Z_{S_0} \cup Z_{\mathrm{rad}_\Omega}, Z_2 \cup Z_{\mathrm{rad}_{\Gamma_2}}, Z_1 \cup Z_{\mathrm{rad}_{\Gamma_1}}, \Gamma_2(Z_2)\right) \qquad (47)$$

Indeed, $\mathbf{A}_{21}$ multiplied by equation (46) can be understood as the pressure coming from Γ_1 radiating towards Γ_2 with the needed impedances. Particularly, the "internal" impedance of Γ_1 and the pressure on Γ_1 are united in the existence of source S_{21}, so the right-hand term of equation (46) can now be understood as the source pressure

$$\mathbf{g}_{21}\left(Z_{S_0} \cup Z_{\mathrm{rad}_\Omega}, Z_2 \cup Z_{\mathrm{rad}_{\Gamma_2}}, \Gamma_1(Z_1)\right) \qquad (48)$$

Upon multiplication by $\mathbf{A}_{12}$, (48) becomes

$$\mathbf{g}_{21}\left(Z_{S_0} \cup Z_{\mathrm{rad}_\Omega}, Z_2 \cup Z_{\mathrm{rad}_{\Gamma_2}}, Z_1 \cup Z_{\mathrm{rad}_{\Gamma_1}}, \Gamma_2^{\mathrm{geom}}\right) \qquad (49)$$

and finally via $[\mathbf{I} - \mathbf{A}_{22}]^{-1}$

$$\mathbf{g}_{21}\left(Z_{S_0} \cup Z_{\mathrm{rad}_\Omega}, Z_2 \cup Z_{\mathrm{rad}_{\Gamma_2}}, Z_1 \cup Z_{\mathrm{rad}_{\Gamma_1}}, \Gamma_2(Z_2)\right) \qquad (50)$$

Each impedance grouping is linked to a particular propagation path, so there are as many reflections as groupings. The interpretation of all other terms follows the same procedure. But even if these conclusions give meaning to the image sources and to the number of reflections that are associated with them, they still remain to be formally demonstrated. For it is at first sight

surprising that an incident pressure wave on a wall would lead to a source pressure as soon as the wall impedance is considered *and* that this very impedance would be considered *a second time* when this source radiates (again, part (*) of equation (44) shows a combination of this wall impedance and the radiation impedance).

C. Integral representation inside the domain and series development

The investigation proposed in this paper of the rational origins of the notion of image sources associated with the acoustical ray method rests entirely on the series development of the exact solution of the wall pressure. This development could not have been directly applied to the exact solution within the domain. Whereas, now that the wall pressure can be developed as a series, an extension toward an expression of the pressure inside the domain is possible. Only the case of perfectly reflecting walls is considered here. Again, some preliminary remarks are needed.

In the elementary configuration of Figure 6a, pressure at point R is expressed by

$$p(R) = G_\infty(R,S) + \underbrace{\int_\Gamma p(M)\partial_{n_M} G_\infty(M,R)dM}_{\text{contribution from S', or } G_\infty(R,S')} \tag{51}$$

with (according to (4))

$$p(M) = G_\infty(M,S) + G_\infty(M,S') = 2G_\infty(M,S') \tag{52}$$

thus leading to the following matrix equation (with our notation conventions)

$$\mathbf{p} = \mathbf{g}(\Omega) + \mathbf{E}_\infty \cdot \mathbf{p}(\Gamma) = \mathbf{g}(\Omega) + \mathbf{E}_\infty \cdot 2\mathbf{g}'(\Gamma) \tag{53}$$

For the two-walled configuration under study here (Figure 6b), we write similarly

$$\mathbf{p} = \mathbf{g_0}(\Omega) + \mathbf{E_1} \cdot \mathbf{p_1} + \mathbf{E_2} \cdot \mathbf{p_2} \tag{54}$$

During the analysis of the series development to obtain the source contribution, it appears that the terms are counted by pairs. Indeed, the formulation is also

$$
\begin{aligned}
\mathbf{p} = \mathbf{g_0}(\Omega) \;+\; \mathbf{E_1}.(&\underbrace{\mathbf{g_0}(\Gamma_1) + \mathbf{g_1}(\Gamma_1)}_{2\,\mathbf{g_1}(\Gamma_1)} + \underbrace{\mathbf{g_{12}}(\Gamma_1) + \mathbf{g_{121}}(\Gamma_1)}_{2\,\mathbf{g_{121}}(\Gamma_1)} + \underbrace{\mathbf{g_{1212}}(\Gamma_1) + \mathbf{g_{12121}}(\Gamma_1)}_{2\,\mathbf{g_{12121}}(\Gamma_1)} + ...) \\
+\; \mathbf{E_1}.(&\underbrace{\mathbf{g_2}(\Gamma_1) + \mathbf{g_{21}}(\Gamma_1)}_{2\,\mathbf{g_{21}}(\Gamma_1)} + \underbrace{\mathbf{g_{212}}(\Gamma_1) + \mathbf{g_{2121}}(\Gamma_1)}_{2\,\mathbf{g_{2121}}(\Gamma_1)} + \underbrace{\mathbf{g_{21212}}(\Gamma_1) + ...}_{2\,\mathbf{g_{21212}}(\Gamma_1)} + ...) \\
+\; \mathbf{E_2}.(&\underbrace{\mathbf{g_0}(\Gamma_2) + \mathbf{g_2}(\Gamma_2)}_{2\,\mathbf{g_2}(\Gamma_2)} + \underbrace{\mathbf{g_{21}}(\Gamma_2) + \mathbf{g_{212}}(\Gamma_2)}_{2\,\mathbf{g_{212}}(\Gamma_2)} + \underbrace{\mathbf{g_{21212}}(\Gamma_2) + \mathbf{g_{212121}}(\Gamma_2)}_{2\,\mathbf{g_{212121}}(\Gamma_2)} + ...) \\
+\; \mathbf{E_2}.(&\underbrace{\mathbf{g_1}(\Gamma_2) + \mathbf{g_{12}}(\Gamma_2)}_{2\,\mathbf{g_{12}}(\Gamma_2)} + \underbrace{\mathbf{g_{121}}(\Gamma_2) + \mathbf{g_{1212}}(\Gamma_2)}_{2\,\mathbf{g_{1212}}(\Gamma_2)} + \underbrace{\mathbf{g_{12121}}(\Gamma_2) + \mathbf{g_{121212}}(\Gamma_2)}_{2\,\mathbf{g_{121212}}(\Gamma_2)} + ...)
\end{aligned}
\qquad (55)
$$

Transferring the pressures from the walls towards the domain through $\mathbf{E}_1$ and $\mathbf{E}_2$ leads to

$$\mathbf{p} = \mathbf{g}_0(\Omega) + \mathbf{g}_1(\Omega) + \mathbf{g}_2(\Omega) + \mathbf{g}_{12}(\Omega) + \mathbf{g}_{21}(\Omega) + \mathbf{g}_{121}(\Omega) + \mathbf{g}_{212}(\Omega) + \mathbf{g}_{1212}(\Omega) + ... \quad (56)$$

where assembling terms by pairs always takes into account terms of the same order in the series revealing the pressures on the walls . It must be noted that this particular order of terms is of no significance, and it would have been quite possible to write, for example,

$$\mathbf{p} = \mathbf{g}_0(\Omega) + \mathbf{g}_2(\Omega) + \mathbf{g}_1(\Omega) + \mathbf{g}_{12}(\Omega) + \mathbf{g}_{21}(\Omega) + \mathbf{g}_{212}(\Omega) + \mathbf{g}_{121}(\Omega) + ... \qquad (57)$$

However, in the present case, the relative order of the terms series stemming from S_1 and S_2 remains. This question about the order of terms radiating toward the domain will appear in the conclusion.

III - NUMERICAL EXPERIMENTS

The reasoning correlating the terms of the series development and the image sources may lack rigor and an analysis of this reasoning will sooner or later prove necessary, but as a first step, numerical experiments can yield results faster and provide a factual confirmation of the interpretation presented here.

All the experiments presented here were done in the situation depicted in Figure 7, composed of two perfectly reflecting walls Γ_1 and Γ_2, at an angle θ. The present study is

concerned with the justification of a possible term-by-term relation between the series development of the integral solution and the series of image sources. Therefore, work has been concentrated on the case of perfectly reflecting walls (except for Situation B presented in Figure 10, see below), deliberately setting aside the case of absorbing walls. Only after this term-by-term correspondence has been assessed will it be possible to compare a series term with wall impedance and an image source contribution with specular absorption. In this second step, the difference between a local specular reaction and the non-local reaction present in the integral equations (diffusion) could then be verified. Both walls, theoretically of infinite length, are in fact 5m long for numerical reasons; the source is located at the coordinates (x_S, y_S). The values of θ, x_S and y_S used in the different situations referred to in this section are summed up in Table I. The walls are discretized into 250 facets of a length of 0.02m each (the wavelength is ca. 0.7m). The pressure is computed on both walls at 500 Hz. In the following tests, the solution obtained by the image sources method is compared with the corresponding series development. The reference solution in all cases is computed with the integral method. This solution is assumed to be exact, but with an approximation brought by the discretization and the finite length of the walls.

Seeking a way to observe if there is a correspondence between the terms of the series development and the image sources for the computation of the wall pressure, the first test comes from an intuitive consideration. For an acute angle θ, a great number of reflections can occur between the walls, so a great number of image sources is expected; it is noticeable that the image choice algorithm shows that all image sources are visible for the wall pressure. For $\theta > \pi/2$ (obtuse), a small number of sources should intervene. It could be that the number of image sources is a monotonous function of the angle, so the convergence speed of the series should

increase from acute to obtuse angles. To verify this assertion, a distance between the exact solution (actually the expression "exact" is incorrect since the solution is only numerically approached) and the solution obtained with a number N_t of terms of the series development or obtained with a number N_s of image sources is defined as

$$d(N_t)=\int_{\Gamma_1}\left|p_{series}(N_t,x)-p_{exact}(x)\right|^2 dx \quad \text{and} \quad d(N_s)=\int_{\Gamma_1}\left|p_{sources}(N_s,x)-p_{exact}(x)\right|^2 dx \quad (58)$$

Figure 8 shows that the convergence curves of both the ray method and series development solutions are closely related and verify the fact that the convergence is faster for wider angles. For acute angles, the extra terms of the series development (those without an image source equivalent) appear to be of weak or even negligible contribution compared to the first terms. From a more physical point of view, the development series and its interpretation *via* Huygens' Principle lead to the same conclusion, since the specular part of the sound field (located in the first terms of the series) is of greater importance than the diffracted part (in the higher order terms). Therefore the correspondence between the terms of the series development and the image sources can be further explored. Let us remark that in the case of an open sector, no resonances with infinite amplitudes at some frequencies are expected, which has indeed been observed.

A special situation is the so-called quarter-infinite space (in 2D), where $\theta=\pi/2$ (situation A). It has been previously observed that the image source method is in very good agreement with the reference solution in the case of perfectly rigid walls and also of those with a local impedance [13]. This also means that the visible sources (of which there are 4: the real source plus 3 images) contain the majority if not all of the needed information. Figure 8 shows that the reference solution is reached in four terms both by the series development and by the corresponding image sources. However, a closer observation (induced by the strong

convergence, as we shall see) shows a very slight difference between the two convergence curves: the terms of the series development converge a little more slowly than the sum of the image sources contributions. This could be due to the numerical approximation of the exact (reference) solution, and will be further examined. This situation where the first four terms are sufficient to obtain a good solution ought to be revealed in equation (23) if the product of the matrices $\mathbf{C}\cdot\mathbf{B}$ were null for $\theta=\pi/2$ without $\mathbf{B}$ or $\mathbf{C}$ being zero. In practice, this would be highlighted by a norm of the product. Figure 9 shows the maximum singular value of the product $\mathbf{C}\cdot\mathbf{B}$ along with the convergence (according to (58)) of the 5th term of the series development on Γ_1, i.e. $2\mathbf{C}\cdot 2\mathbf{B}\cdot\mathbf{g_0}(\Gamma_1)$. Both values are seen to decrease from acute angles toward $\pi/2$. The convergence stabilizes at zero from there on, signifying that the 5th term is superfluous for obtuse angles. On the other hand, the fact that the maximum singular value of $\mathbf{C}\cdot\mathbf{B}$ is not null at $\theta=\pi/2$ could hint that this norm is perhaps not appropriate to treat the expected vanishing of $\mathbf{C}\cdot\mathbf{B}$ at $\theta=\pi/2$.

Despite the fact that the numerical experiments presented in this paper focus on the case $\beta = 0$, to gain confidence in the well-founded base of the work, a comparison is proposed in Figure 10 between the pressure field on the boundaries of a quart-infinite space (situation B) with an arbitrary impedance (reduced impedance $Z_r = 9$, which characterises an absorption of about 36% at normal impedance) calculated with the integral method and the pressure calculated with the four images. The very good agreement between both fields lead us to believe that the first four terms of the series still correspond to the four sources, probably resulting therefore in product $\mathbf{D}_{12}\cdot\mathbf{D}_{21}$ in equation (39) null without both of the matrices being zero, but this still remains to be demonstrated.

The weak convergence in Figure 8 for an acute angle θ shows that the interpretation of the series development proves coherent at first sight and hints at a formal justification of the image sources method, but offers no improvement of this method, since the extra terms (not corresponding to visible sources) are of negligible contribution. On the contrary, for obtuse angles one can show the effects of adding the "supplementary" sources, coming from the terms of the series development without a "real" corresponding image source ("invisible" source as mentioned in Figure 2b). To show the impact of this extra source, two situations, showing characteristic features of the method, are displayed here. The situations considered are as defined in Table I. Figure 11a (situation C) shows an increase in precision when an extra source (in this case S_2) is added. For another situation, however, Figure 11b (situation D) seems to show that adding a source can indeed weaken the solution. This puts the distance as defined above into question and leads to the observation of the strong convergence, i.e. the comparison between the actual pressure levels obtained by each method. The horizontal lines in Figure 11 occur when no additional sources are considered.

Instead of observing a mean value between the reference solution and the computed one, the actual pressure level on each point of the wall is observed. Figure 12a shows the strong convergence in the case of acute θ (situation F). The terms of the series development can be seen to converge toward the exact solution. In Figure 12b, a more detailed view shows the first 6 terms and their corresponding image sources. An almost perfect coherence between the terms and the sources can be observed. This is expected for the first two terms, since they are conceptually identical, but the coherence of the higher terms is significant for the validity of the interpretation.

As said earlier for $\theta=\pi/2$, the series development converges more slowly than the sum of the image sources contributions. Figure 13 shows the strong convergence for situation A, which has $\theta=\pi/2$ and confirms this remark, for only 4 image sources are necessary to converge toward the reference solution, whereas 6 series development terms are needed (although 4 terms already lead to a very acceptable result).

Observing the pressure level on the walls (strong convergence) for cases with an obtuse angle θ (situation C in Figure 14a, D in Figure 14b and E in Figure 14c) reveals the enhancement brought about by adding an extra invisible source (in this case S_2). The oscillatory behaviour of the wall pressure is not taken into account if only the visible sources are used. This valuable information is added when an extra source is used (but was not accessible when only observing the weak convergence, as in Figure 11b).

IV – CONCLUSION

The acoustic ray method rests upon specular reflection – combined with the notion of associated image sources in one version of the method – that has been intuitively accepted following geometrical optics. Sound fields in cavities have thus been computed and the results compared with finite element method results, shedding light on differences between the two methods, which we seek to reduce. Acoustic rays, not taking diffraction into account, will always show different results. Nevertheless, and having a possible improvement of the ray method in mind, the primary goal of this research was to identify the analytical origin of image sources and so tackle the problem in a rational way.

For this purpose, the analysis of the exact solution of the harmonic wall pressure in an elementary domain (angular sector in 2 dimensions, bounded by two “walls”, totally reflective to

start with, and then absorbent) has brought interesting results. Of particular interest was the generalization of the notion of image sources, of which some that are normally not considered in the classical image source method could lead to better results, were they used. In fact, the exact solution (obtained by an integral representation of the problem) can be developed into a series after being discretized and written in matrix form. Thanks to Huygens' Principle, the first terms of this series could represent the contributions of the image sources that are given by the method currently used. The other terms in the series would then be represented by generalized image sources. Such sources are actually missing in the classical ray method and could be used to refine the sound field computation results. To assert that a particular solution comes closer to a reference solution, a distance has to be defined, in this case an euclydian norm in L^2.

The numerical experiments – where no absorption has been considered at this stage of the investigation, except for a short illustration – have greatly confirmed the correspondence between the contributions of the first terms of the series development and the corresponding image sources. Moreover, it has been shown that in certain cases, a "missing" image source brings significant extra information (either directly visible with the chosen distance, or visually observable on the graph but not revealed by the chosen distance).

At this level, mentioning the "first" missing source again implies having defined a distance to establish a relation that enables a classification of the image sources' importance. In the configuration proposed in this paper, the euclydian norm used calls "first missing source" the first term of the series that does not correspond to an image source visible at the reception point. As long as this point is located on a wall and at a certain distance from the corners, an idea for the algorithm to make this first missing source appear is envisaged. But the problem requires further investigation for cases where the reception point is near the wall limits.

In the same vein, it has been shown that the acoustic pressure in the domain can also be developed in series, but not immediately. Contrary to the wall pressure case, the order of the terms is in this case still unknown and further research is necessary to identify it. This problem is directly linked to the classification of the influences of walls on the solution at a particular point in the domain. As soon as a rational way to identify these influences is found, physical information on the role of the different walls will be available. This role is for the moment only derived intuitively from simple cases.

Finally, this paper has shown that a solution obtained by current ray methods is an approximation taking into account the first terms of an exact solution obtained via integral representation. But a weak point still remains: ideally the contribution of each source should have been shown to be concentrated in a single series development term, and not spread in multiple terms instead. Nevertheless, this point has been observed in numerical results, although it has not been demonstrated mathematically.

Acknowledgment

This research is supported by the Swiss CTI-7294.1 EUS-IW project within the framework of the European program EUREKA 2790 and is partly funded by *RIETER Automotive Management Corp.* , Winterthur, Switzerland.

REFERENCES

[1] Knudsen, V. O. and Harris, C. M. (**1947**). *Acoustical designing in architecture* (John Wiley & Sons, New York)

[2] Allen, J. and Berkley, D. A. (**1979**). "Image method for efficiently simulating small-rooms acoustics," J. Acoust. Soc. Am. **65**, 943-950

[3] Allard, L., Martin, V. and Rossi, M. (**2000**). "Réponse impulsionnelle d'un contrôleur actif par anticipation dans un semi-espace ; analyse physique et problème de causalité associé" (Impulse response of an active controller by anticipation in half-space ; physical analysis and associated causality problem), Proceedings of the 5th French Congress on Acoustics, Lausanne, Switzerland, 630-631

[4] Krokstad, A., Strom, S. and Sordal, S. (**1968**). "Calculating the acoustical room response by the use of a ray-tracing technique," J. Sound Vib. **8**, 118-125

[5] Kuttruff, H. (**2000**). *Room Acoustics* (4th edition, Spon Press, London)

[6] Jean, P. (**1999**). "Coupling integral and geometrical representations for vibro-acoustical problems," J. Sound Vib. **224**, 475-487

[7] Courtois, T. and Martin, V. (**2004**). "Spectral quality of acoustic predictions obtained by the ray method in coupled two-dimensional damped cavities," J. Sound Vib. **270**, 259-278

[8] Borish, J. (**1984**). "Extension of the image model to arbitrary polyhedra," J. Acoust. Soc. Am. **75**, 1827-1836

[9] Vorländer, M. (**1989**). "Simulation of the transient and steady-state sound propagation in rooms using a new combined ray-tracing/image-source algorithm," J. Acoust. Soc. Am. **86**, 172-178

[10] Mechel, F.M. (**2002**). "Improved mirror source method in room acoustics," J. Sound Vib.

256, 873-940

[11] Martin, V. and Guignard, T. (**2005**). "Justification of the Image Sources in Ray Method," Proceedings of the 12th Int. Congress on Sound and Vibration, Lisbon, Portugal, Paper 178

[12] Baker, B. B. and Copson, E. T. (**1987**). *The mathematical theory of Huygens' Principle* (3rd edition, Chelsea Publishing Company, New York)

[13] Guignard, T., Martin, V. and Courtois, T. (**2004**). "Interpolated identified reflection coefficients for acoustic ray method," Proceedings of the 11th Int. Congress on Sound and Vibration, St. Petersburg, Russia, 3707-3714

Table I - Considered situations

Label	θ	(x_S, y_S) in m	Z_r	Corresponds to Figure
A	$\pi/2$	(3.0, 3.0)	∞	13
B	$\pi/2$	(0.5, 0.5)	9	10
C	$5\pi/8$	(0.5, 2.0)	∞	11a, 14a
D	$5\pi/8$	(-0.5, 2.0)	∞	11b, 14b
E	$7\pi/8$	(0.1, 0.3)	∞	14c
F	$\pi/6$	$(3.0,\ 3.0\cdot\tan(\theta/2))$	∞	12a, 12b

Figure 1 (color online) – Set of image-sources liable to give rise to reflected rays for points in the angular sector; set of rays (i.e., of sources) contributing to the calculation of the acoustic field at point P.

Figure 2 – The implementation of the algorithm for determining the useful image-sources for point Q_1 results in three images in (a) and only one in (b).

Figure 3 – Reflection of an acoustic wave on a totally reflecting plane in the half-infinite space

Figure 4 – Matrices **2B** and **2C** transfer respectively pressure from wall Γ_1 toward wall Γ_2 and inversely.

Figure 5 – Operators $\mathbf{D_{21}}$ et $\mathbf{D_{12}}$ transfer respectively pressure from wall Γ_1 toward wall Γ_2 and inversely (the order of the indices comes from the matrix representation and is to be read from right to left)

Figure 6 – (a) elementary configuration with a reflection on the wall; (b) transfer of pressures from the wall toward the inside of the domain.

Figure 7 – Geometrical configuration for the numerical tests

Figure 8 (color online) – Convergence speed as function of aperture angle θ.

Figure 9 (color online) – The contribution of $\mathbf{C}\cdot\mathbf{B}$ decreases when going from acute to obtuse angles.

Figure 10 (color online) – Pressure levels on wall Γ_1 in situation B, with absorbing walls ($Z_r = 9$)

Figure 11 (color online) – Weak convergence on wall Γ_1: (a) Situation C, (b) Situation D

Figure 12 (color online) - Strong convergence in situation F: (a) convergence of the series development terms toward the exact solution (for clarity, only the first 10 terms are shown); (b) contribution of the first 6 terms of the series development and corresponding image sources.

Figure 13 (color online) - Strong convergence in Situation A

Figure 14 (color online) - Effect of an "invisible" source (a) Situation C, (b) Situation D, (c) Situation E

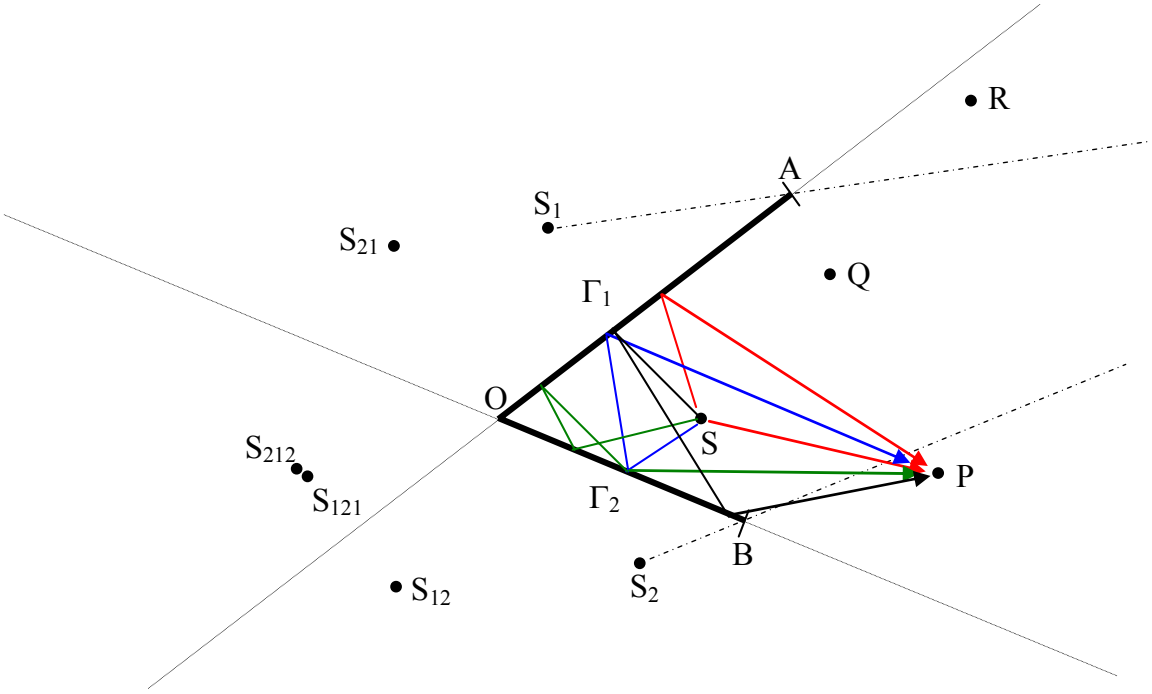
R
A
S1
S21
Q
Γ1
O
S
S212
S121
P
Γ2
B
S12
S2

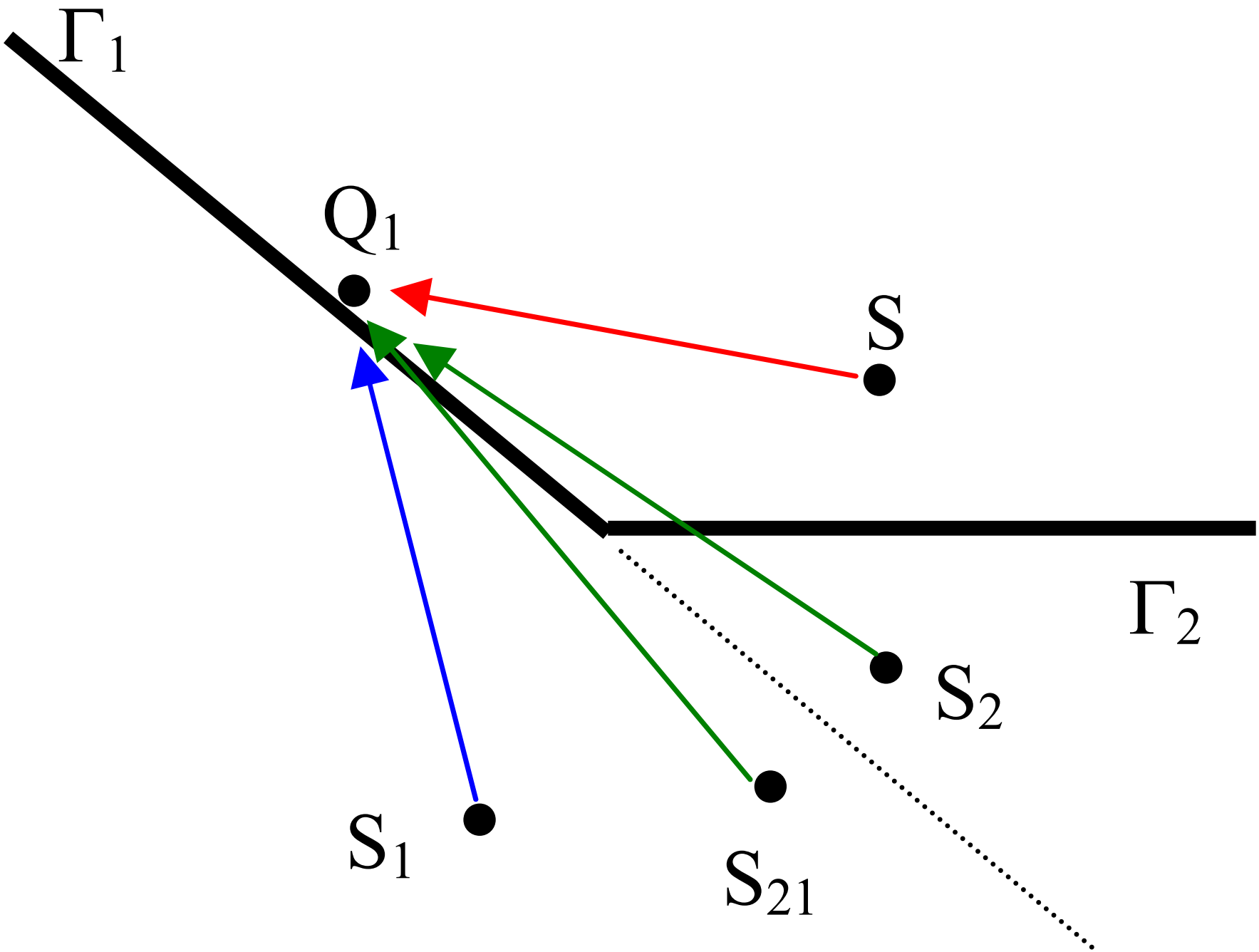
Γ_1
Q_1
S
Γ_2
S_2
S_1
S_{21}

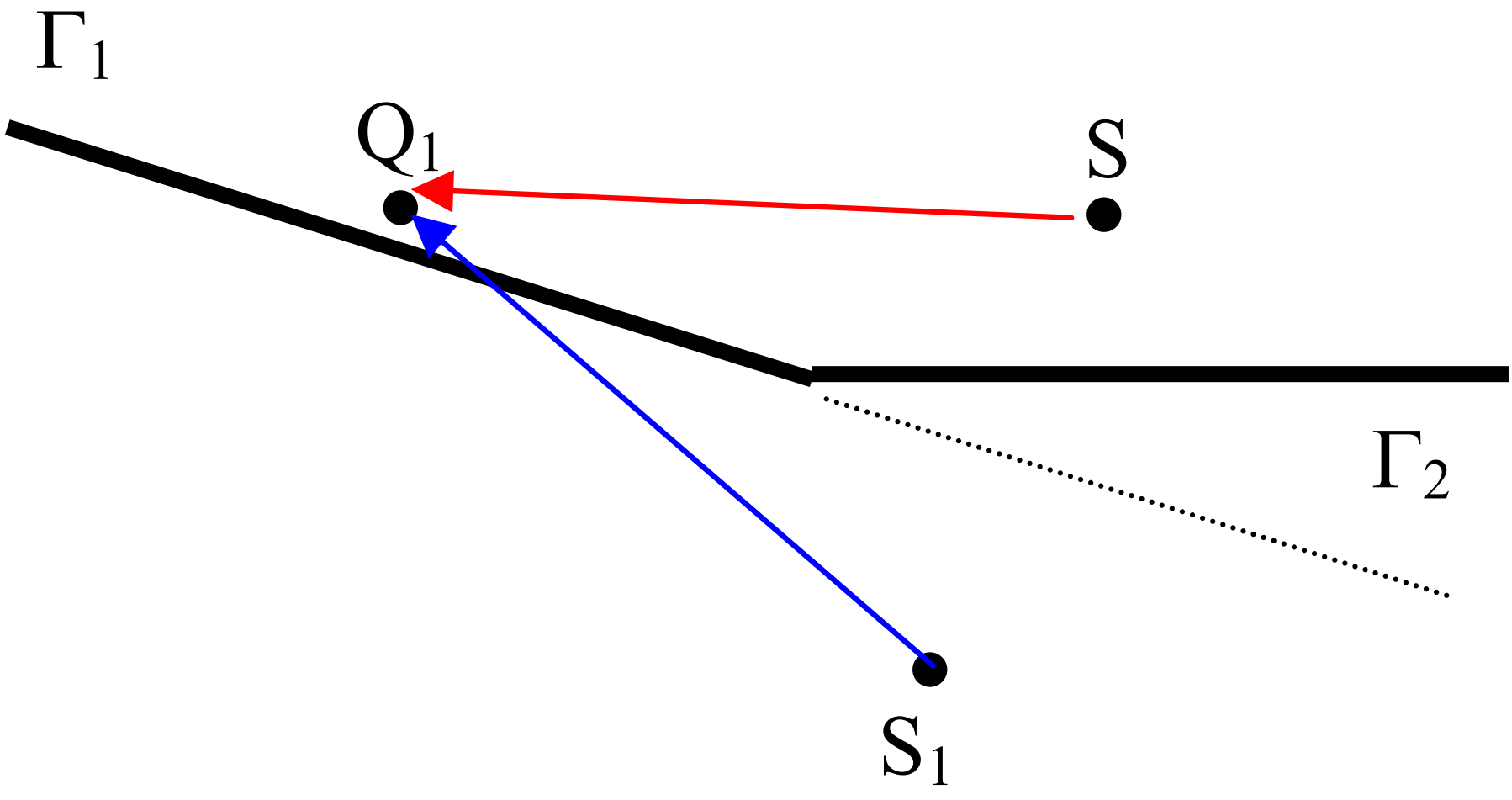
Γ_1
Q_1
S
Γ_2
S_1

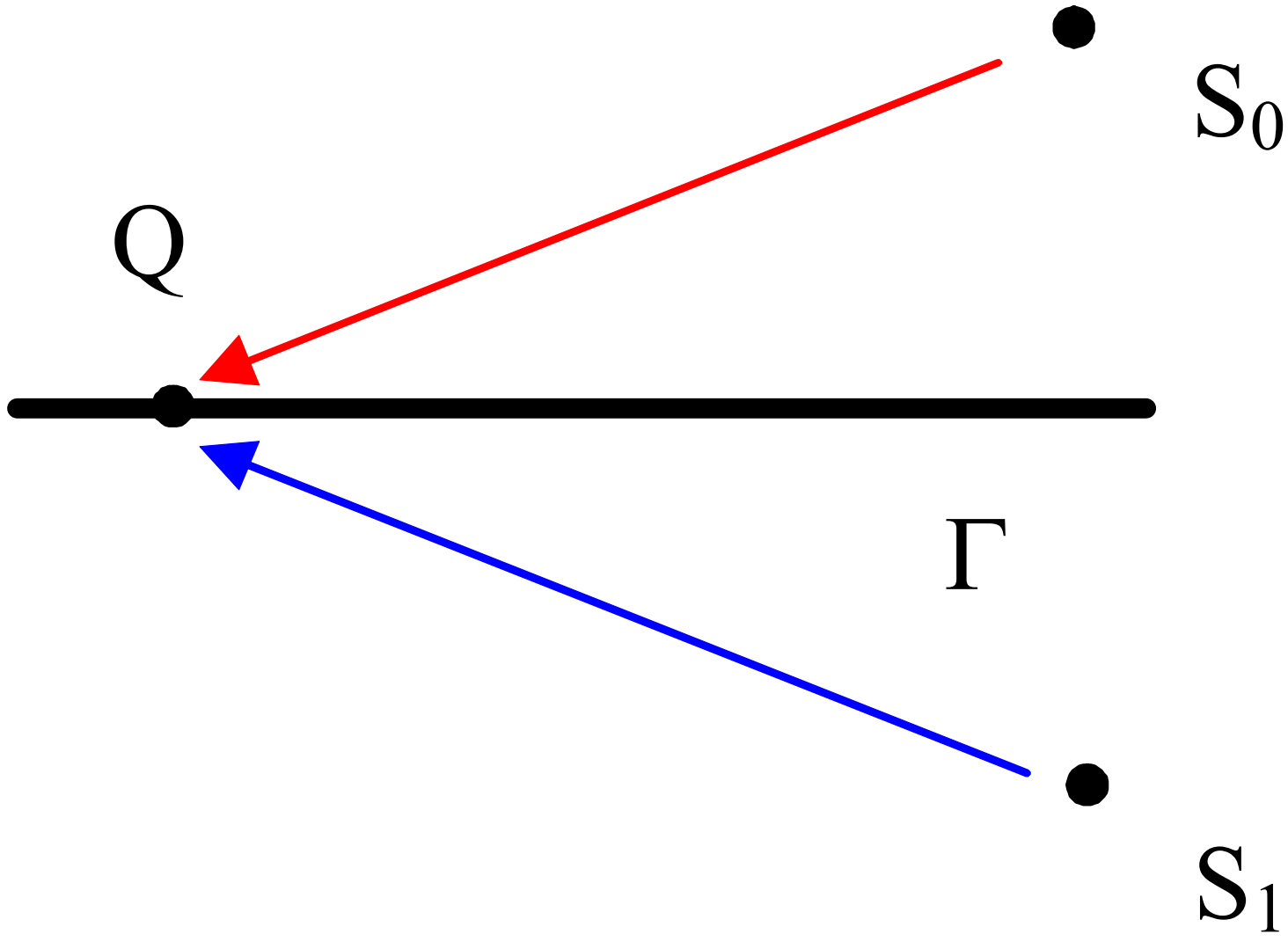
S_0
Q
Γ
S_1

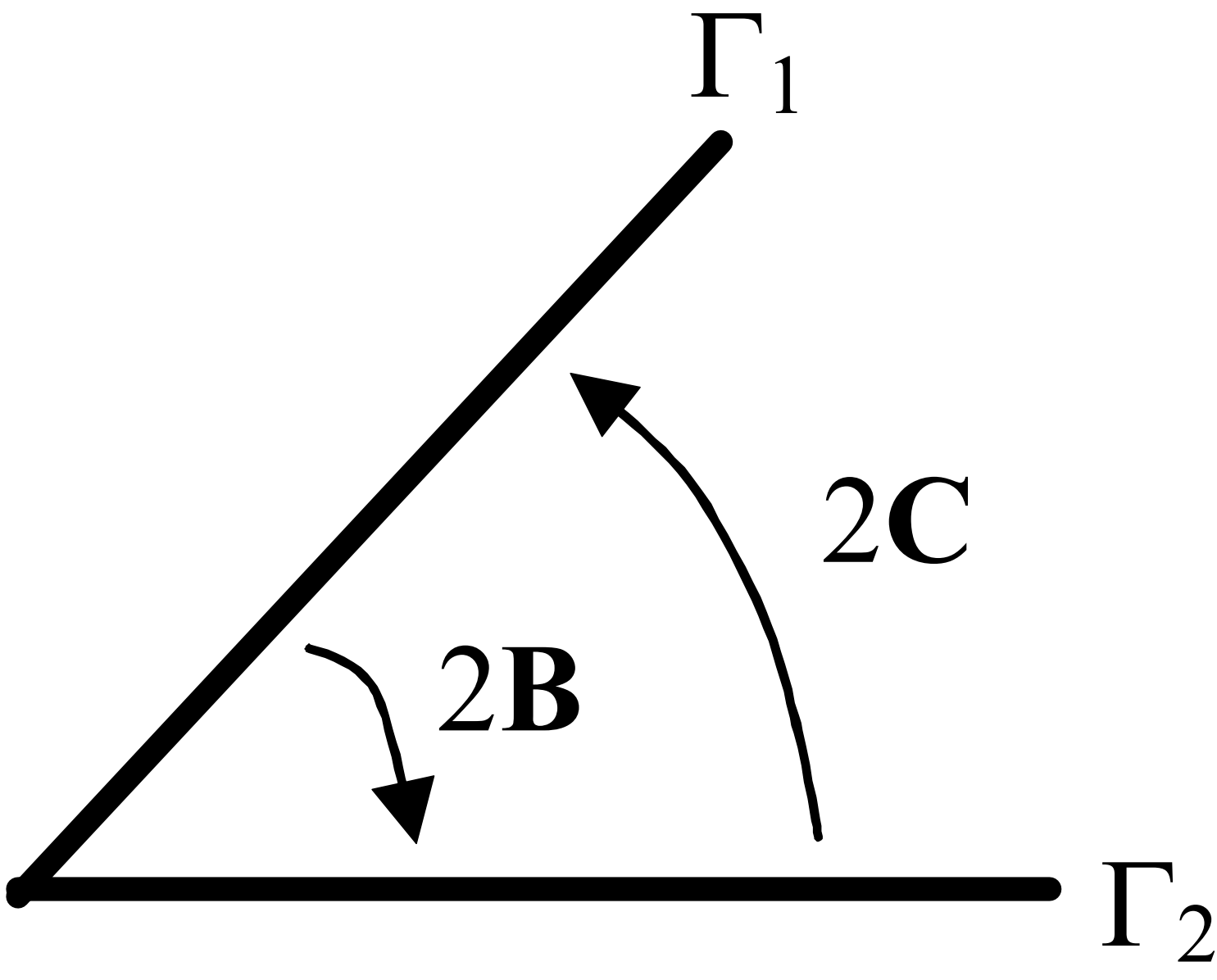
Γ_1
2C
2B
Γ_2

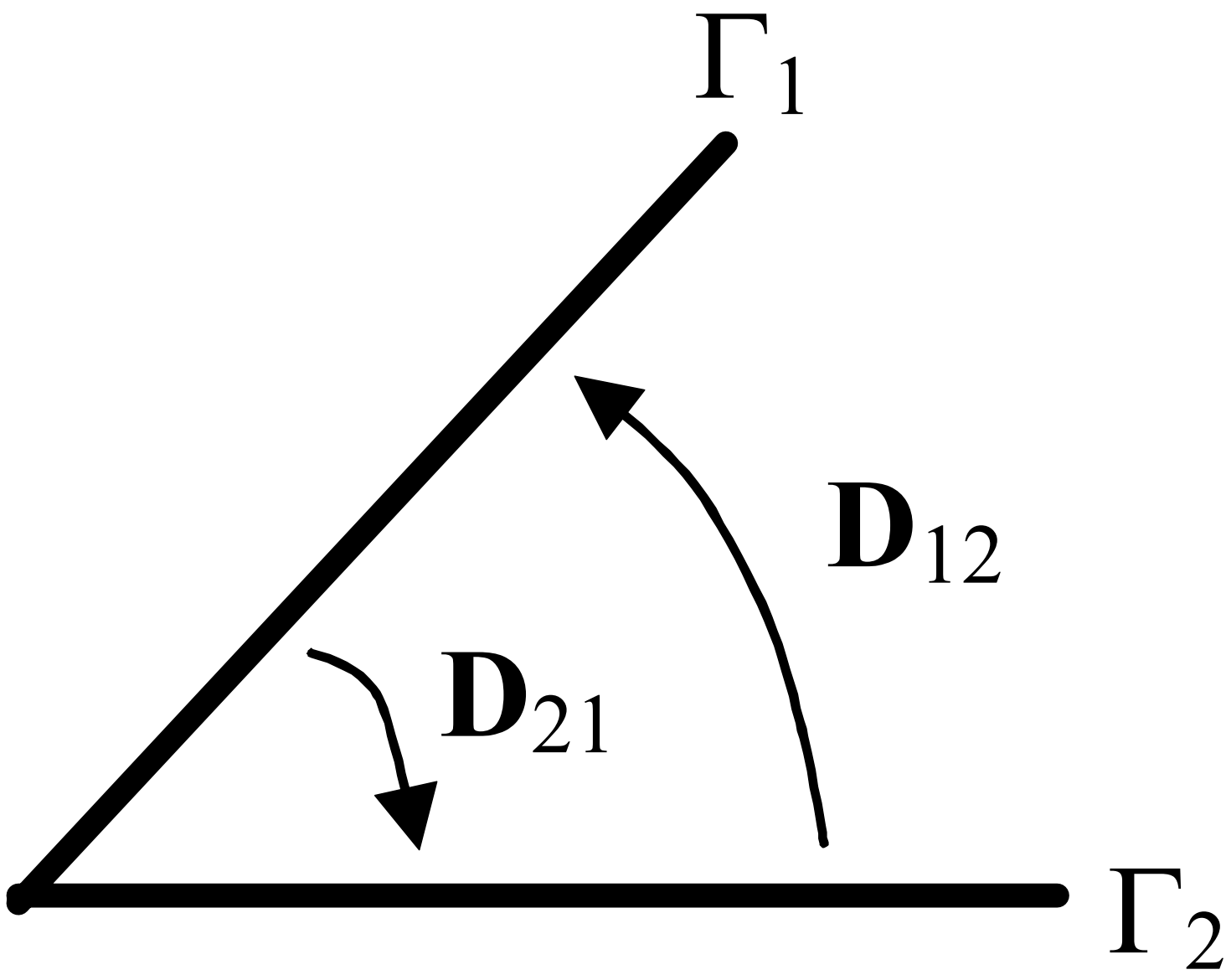
Γ_1
$\mathbf{D}_{12}$
$\mathbf{D}_{21}$
Γ_2

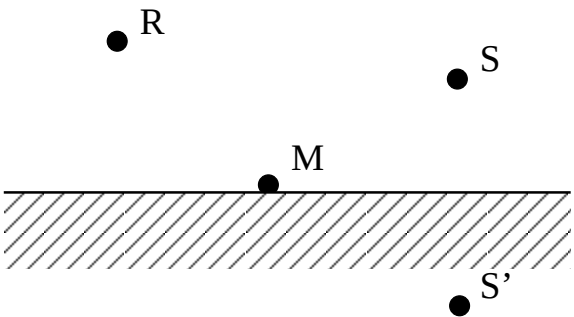
R
S
M
S’

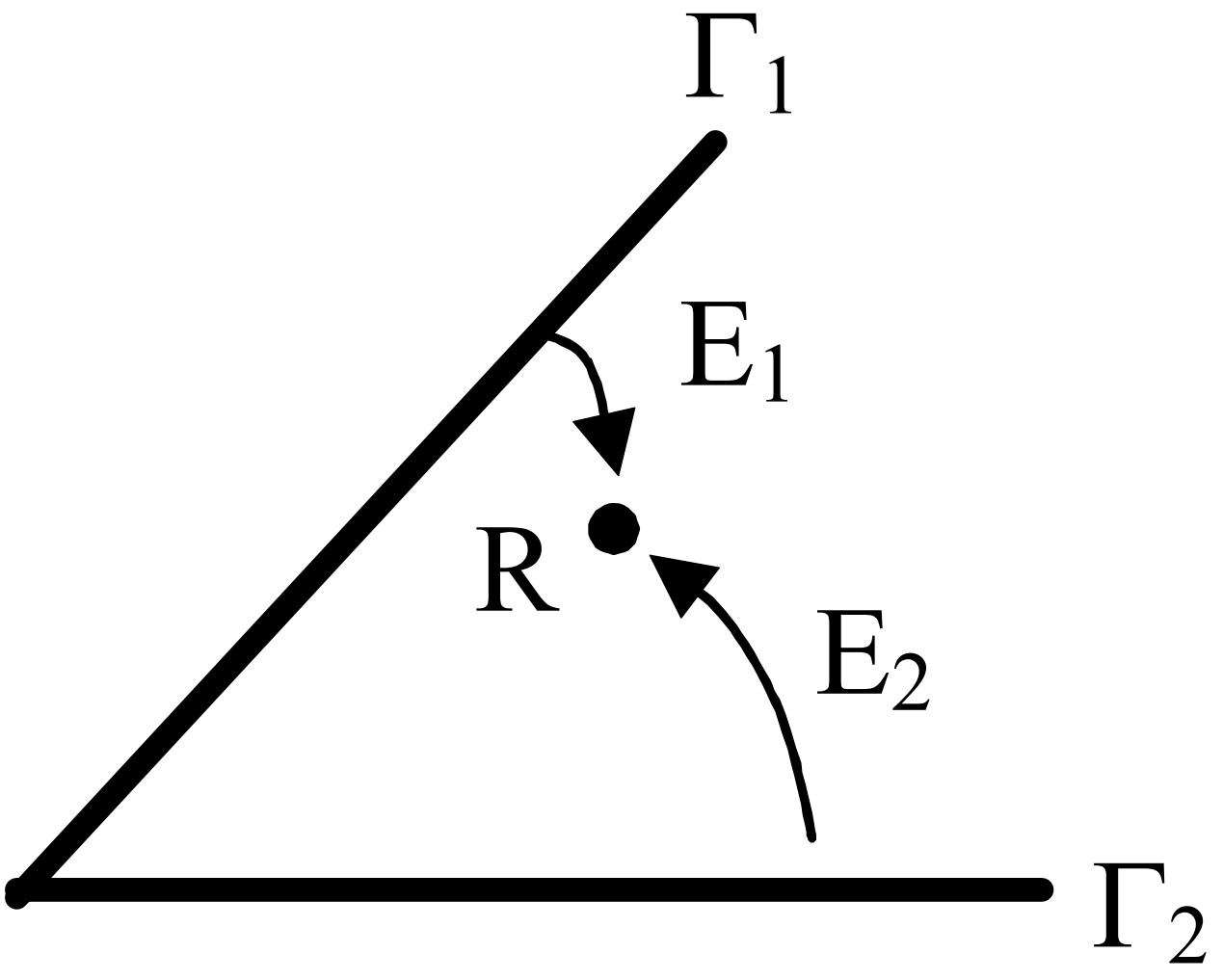
Γ_1
E_1
R
E_2
Γ_2

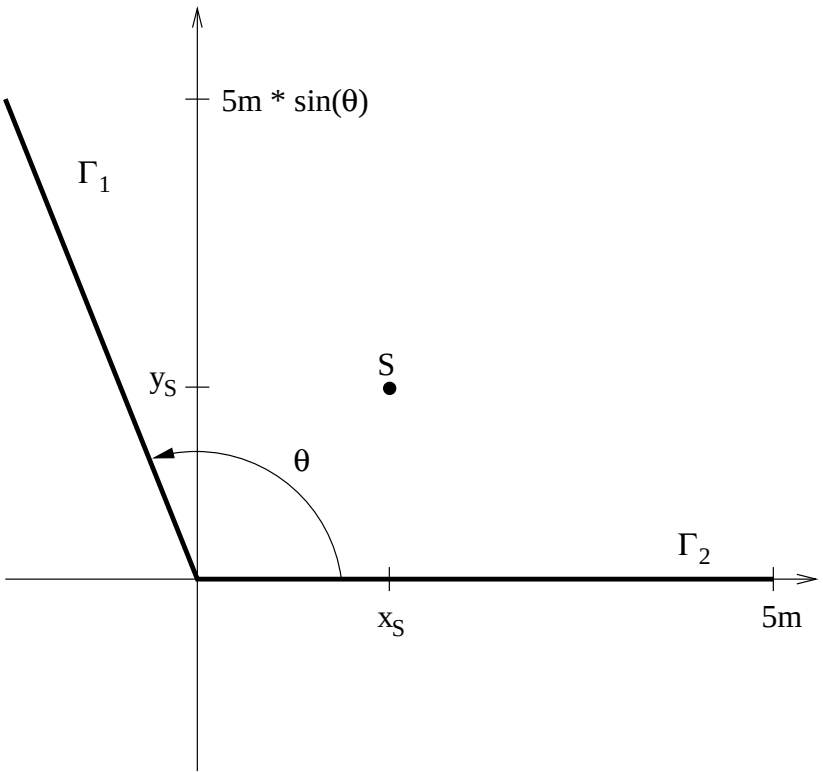
5m * sin(θ)
Γ1
yS
S
θ
Γ2
xS
5m

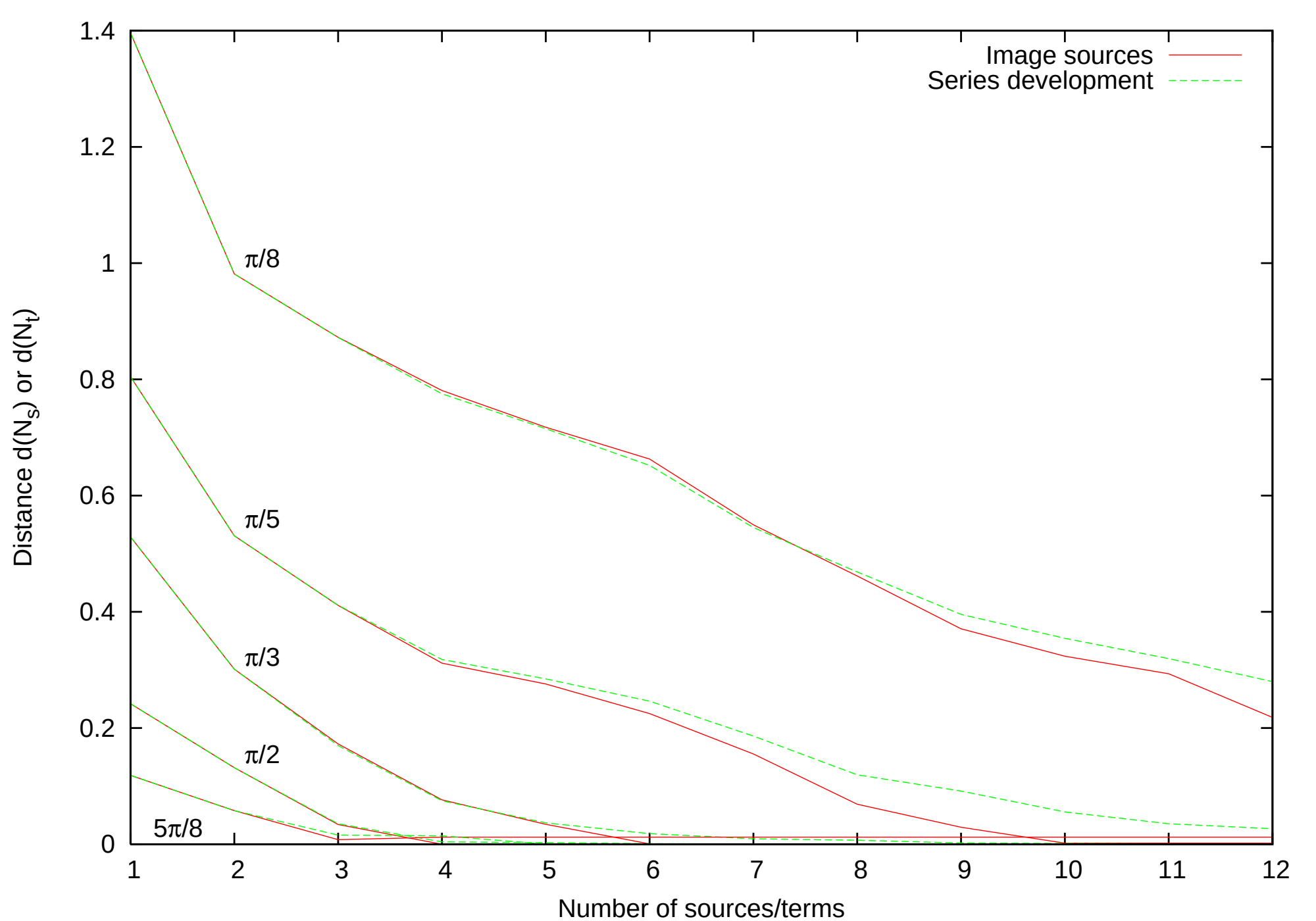
Image sources
Series development
π/8
π/5
π/3
π/2
5π/8
Distance d(N_s) or d(N_t)
Number of sources/terms
1.4
1.2
1
0.8
0.6
0.4
0.2
0
1
2
3
4
5
6
7
8
9
10
11
12

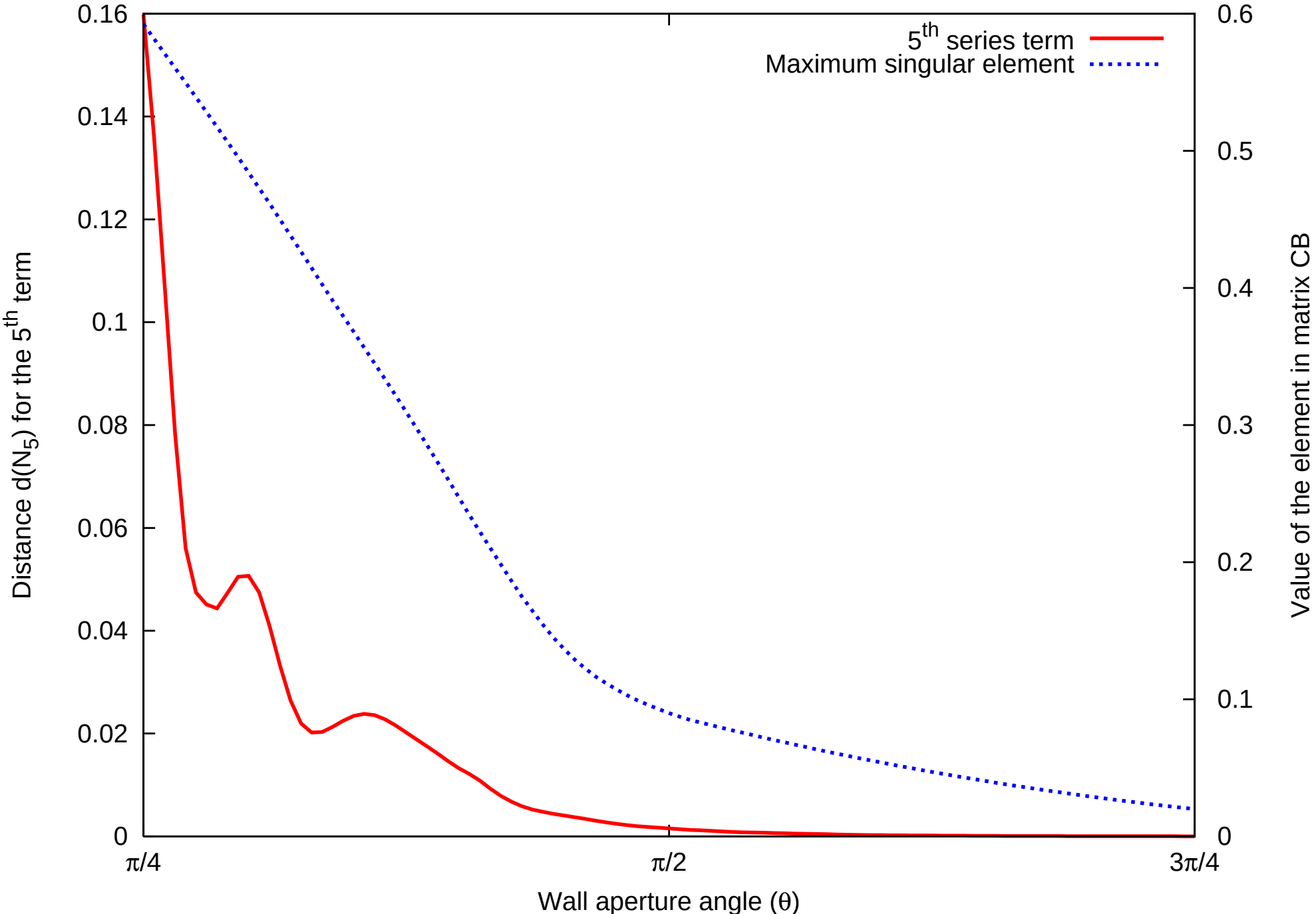
0.16
0.14
0.12
0.1
0.08
0.06
0.04
0.02
0
Distance d(N5) for the 5th term
0.6
0.5
0.4
0.3
0.2
0.1
0
Value of the element in matrix CB
5th series term
Maximum singular element
π/4
π/2
3π/4
Wall aperture angle (θ)

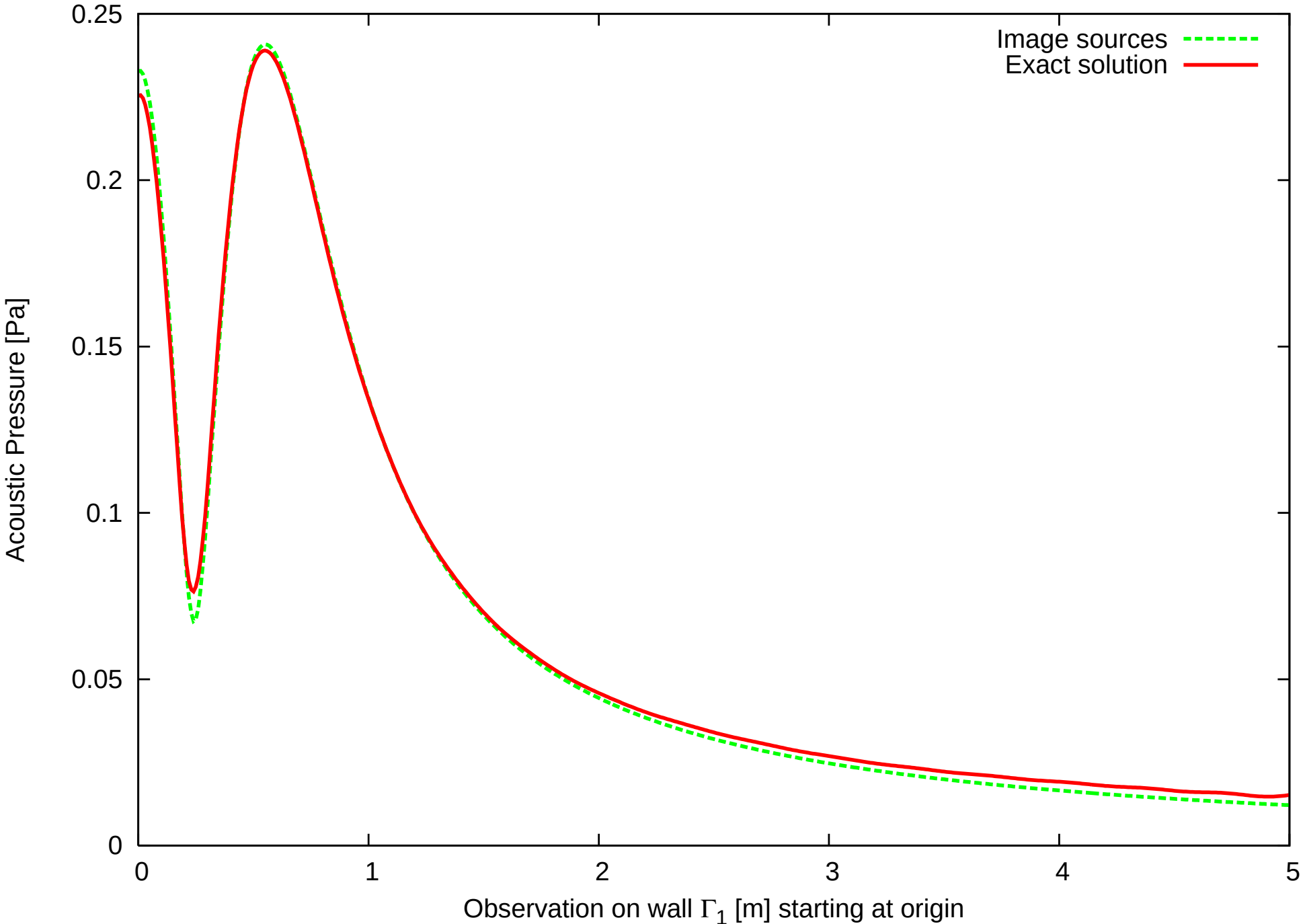
Image sources
Exact solution
Acoustic Pressure [Pa]
0.25
0.2
0.15
0.1
0.05
0
0
1
2
3
4
5
Observation on wall Γ_1 [m] starting at origin

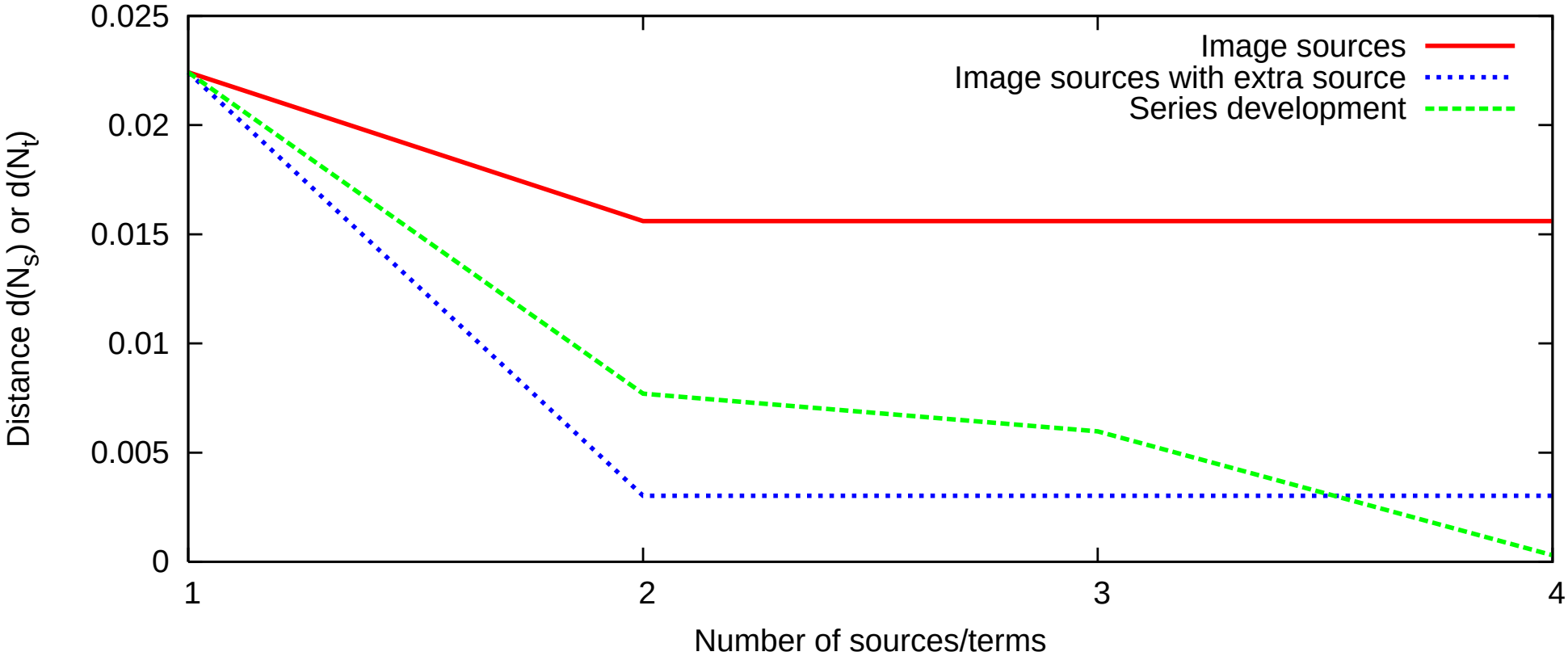
0.025
0.02
0.015
0.01
0.005
0
1
2
3
4
Distance d(N_s) or d(N_t)
Number of sources/terms
Image sources
Image sources with extra source
Series development

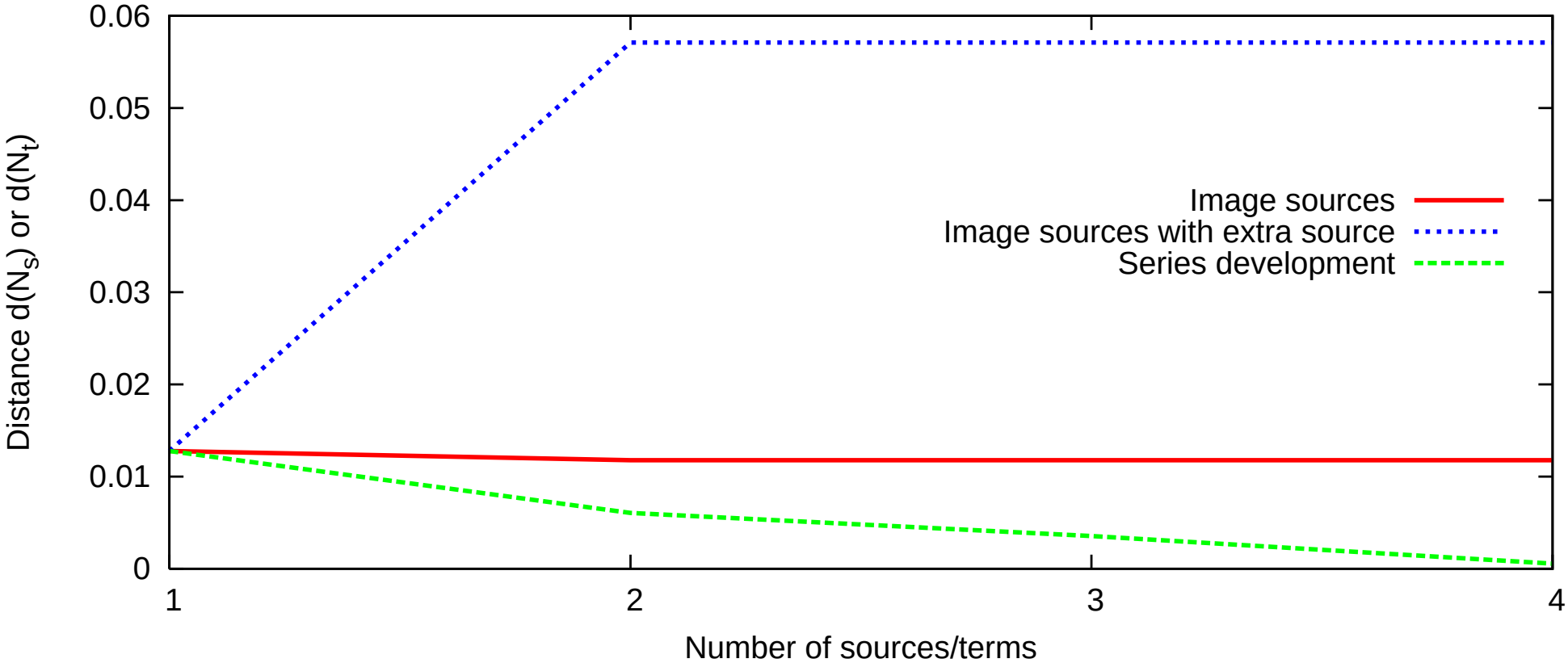
0.06
0.05
0.04
0.03
0.02
0.01
0
1
2
3
4
Distance d(N_s) or d(N_t)
Number of sources/terms
Image sources
Image sources with extra source
Series development

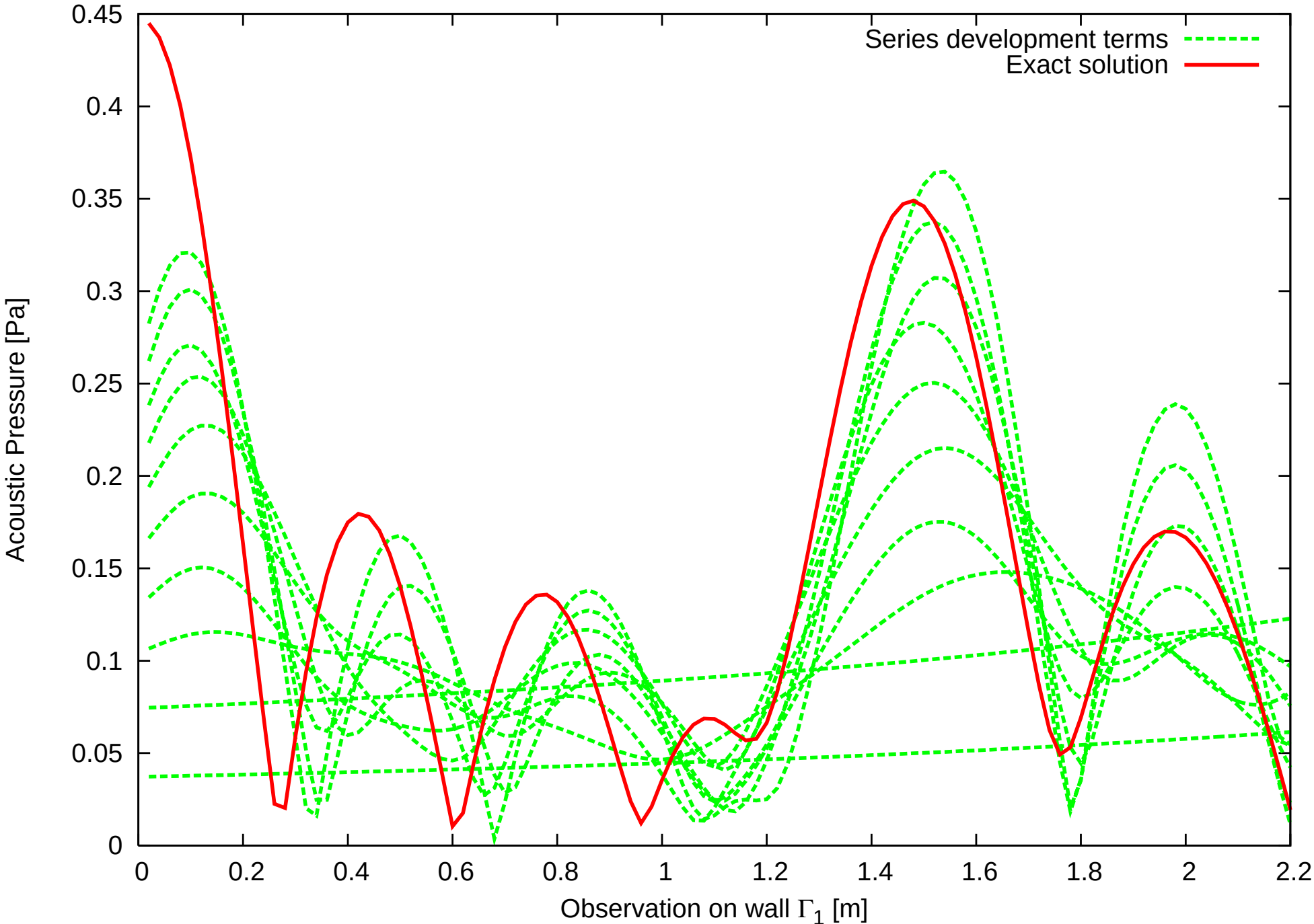
Series development terms
Exact solution
Acoustic Pressure [Pa]
Observation on wall Γ_1 [m]
0.45
0.4
0.35
0.3
0.25
0.2
0.15
0.1
0.05
0
0
0.2
0.4
0.6
0.8
1
1.2
1.4
1.6
1.8
2
2.2

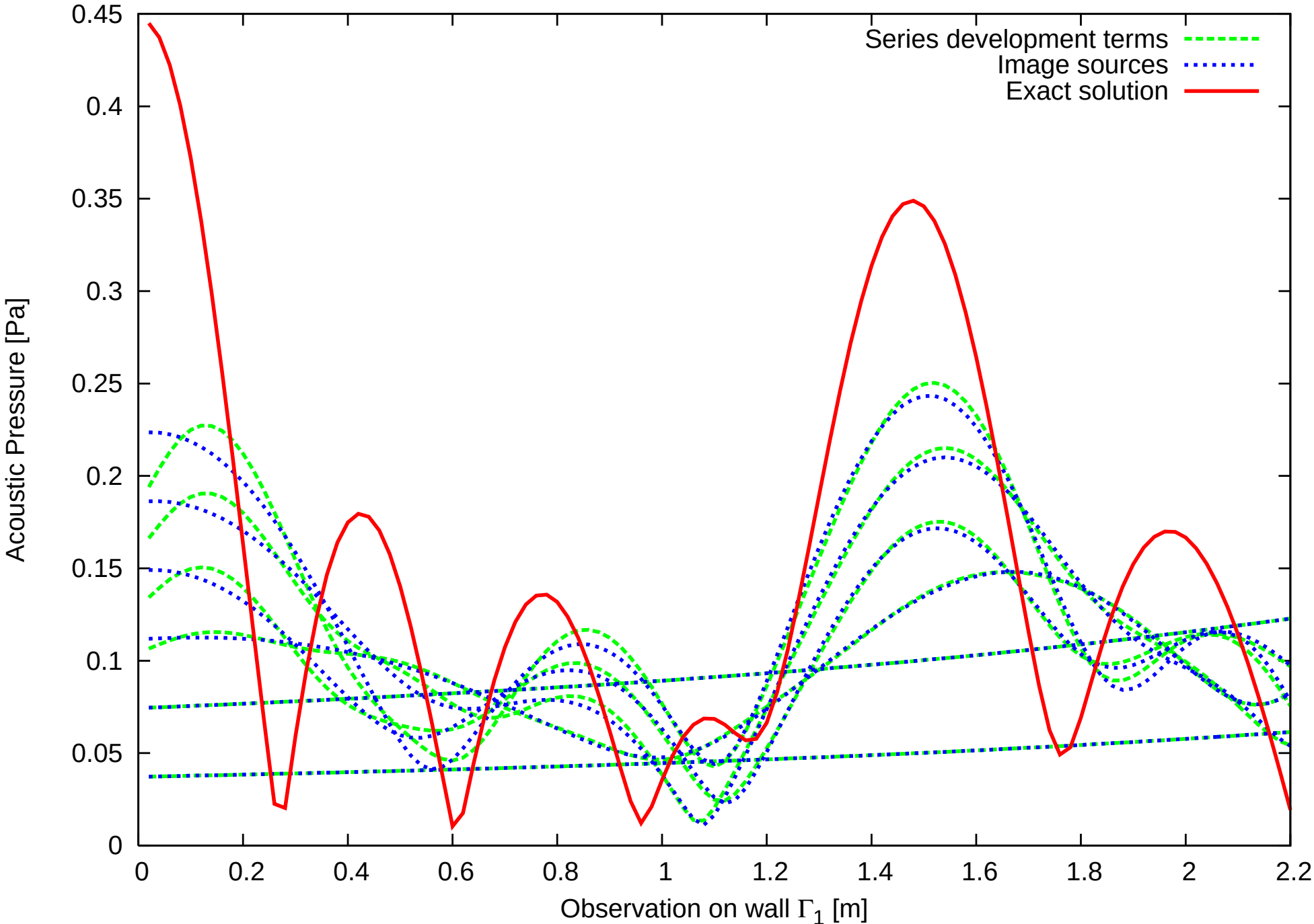
Series development terms
Image sources
Exact solution
Acoustic Pressure [Pa]
Observation on wall Γ_1 [m]
0.45
0.4
0.35
0.3
0.25
0.2
0.15
0.1
0.05
0
0
0.2
0.4
0.6
0.8
1
1.2
1.4
1.6
1.8
2
2.2

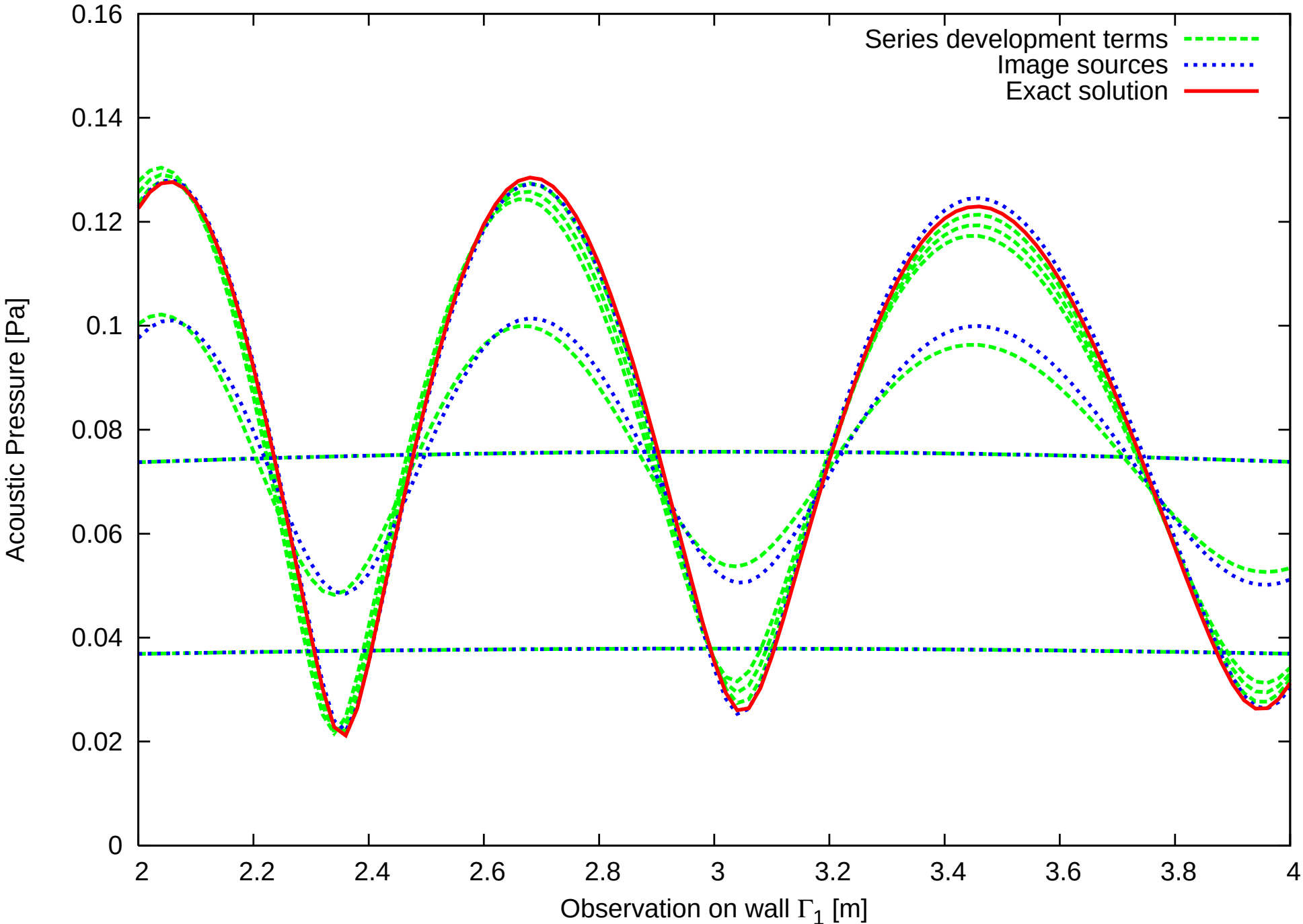
Series development terms
Image sources
Exact solution
Acoustic Pressure [Pa]
Observation on wall Γ_1 [m]
0.16
0.14
0.12
0.1
0.08
0.06
0.04
0.02
0
2
2.2
2.4
2.6
2.8
3
3.2
3.4
3.6
3.8
4

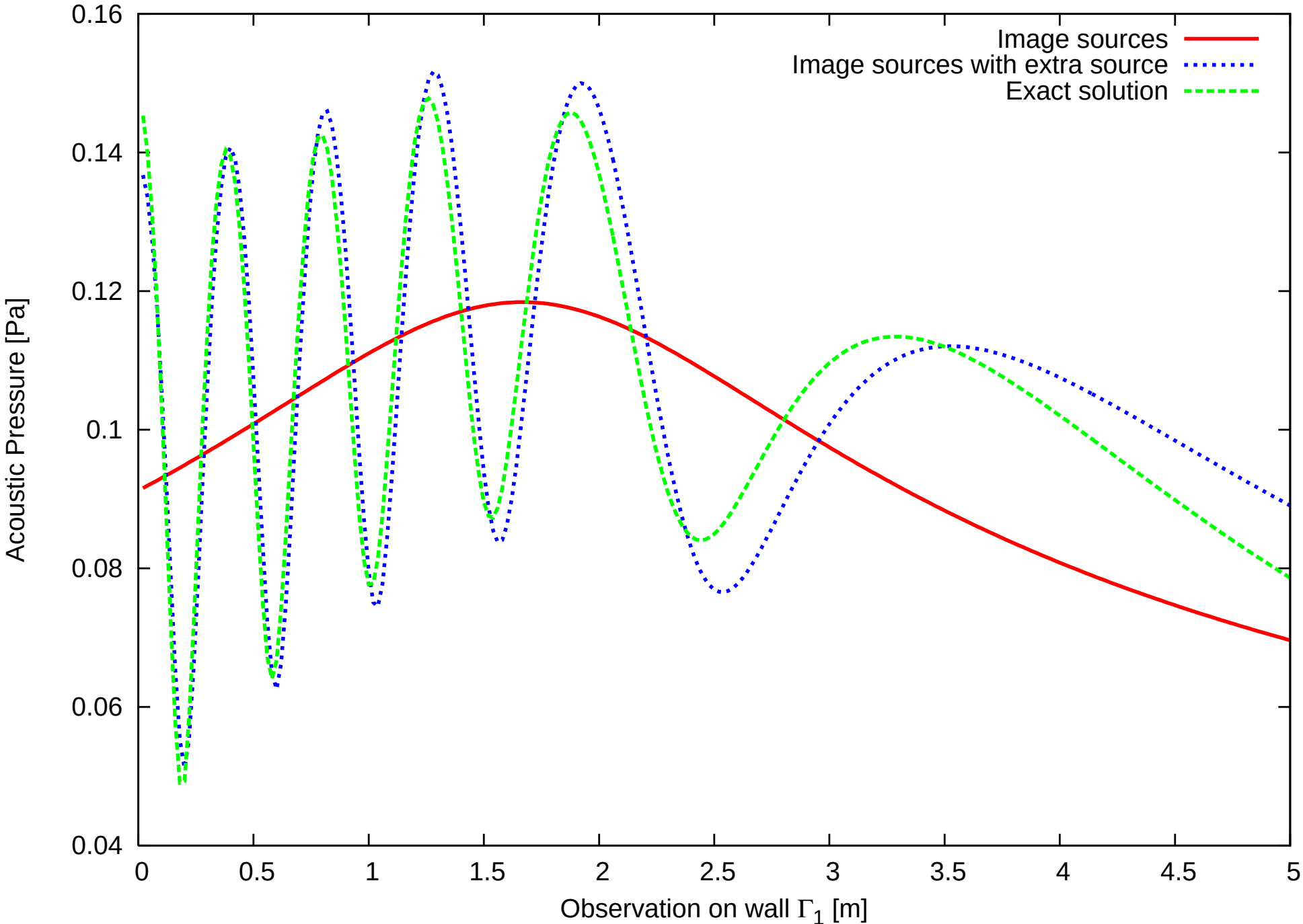
Image sources
Image sources with extra source
Exact solution
Acoustic Pressure [Pa]
0.16
0.14
0.12
0.1
0.08
0.06
0.04
0
0.5
1
1.5
2
2.5
3
3.5
4
4.5
5
Observation on wall Γ_1 [m]

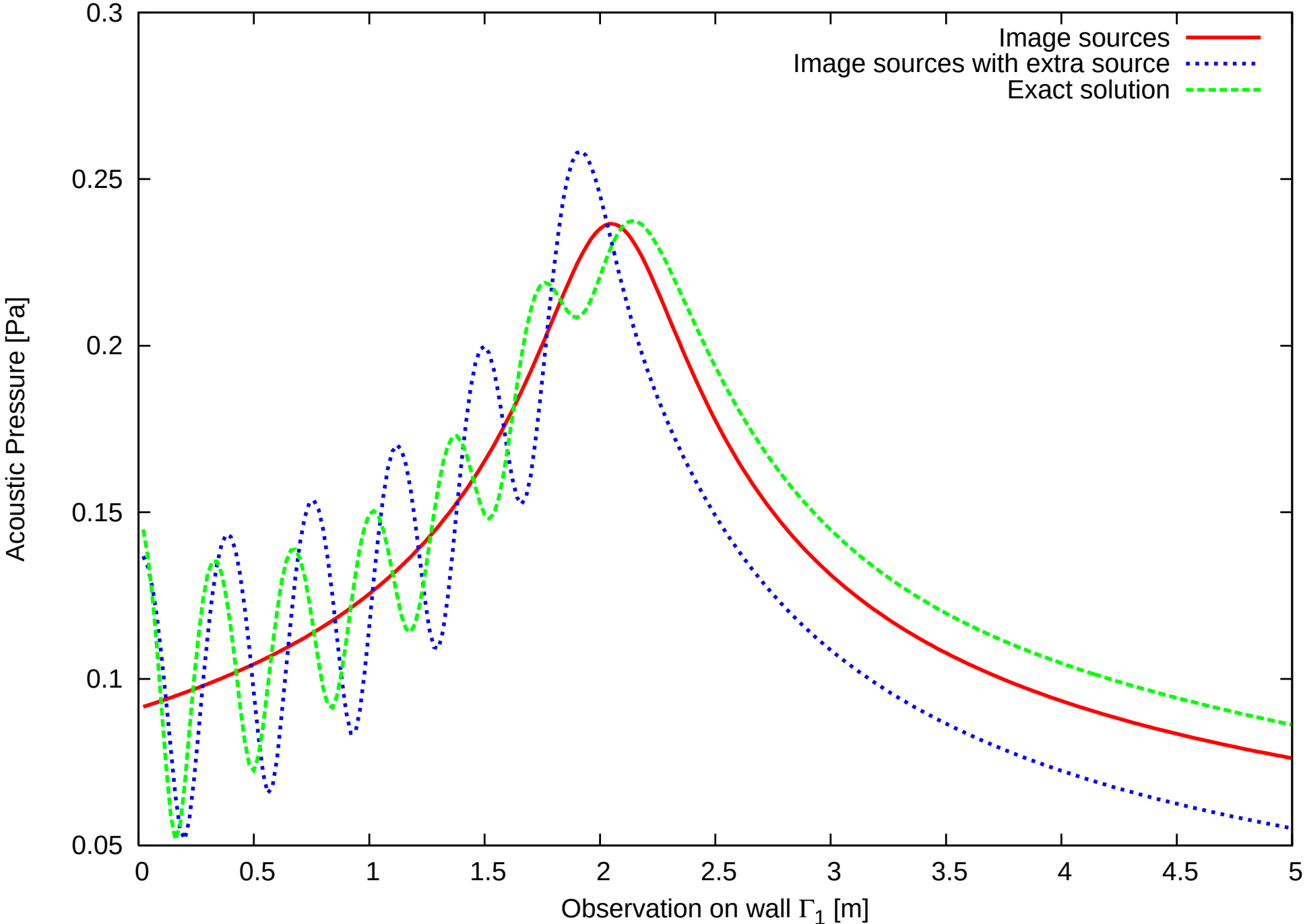
Image sources
Image sources with extra source
Exact solution
Acoustic Pressure [Pa]
Observation on wall Γ_1 [m]
0.3
0.25
0.2
0.15
0.1
0.05
0
0.5
1
1.5
2
2.5
3
3.5
4
4.5
5

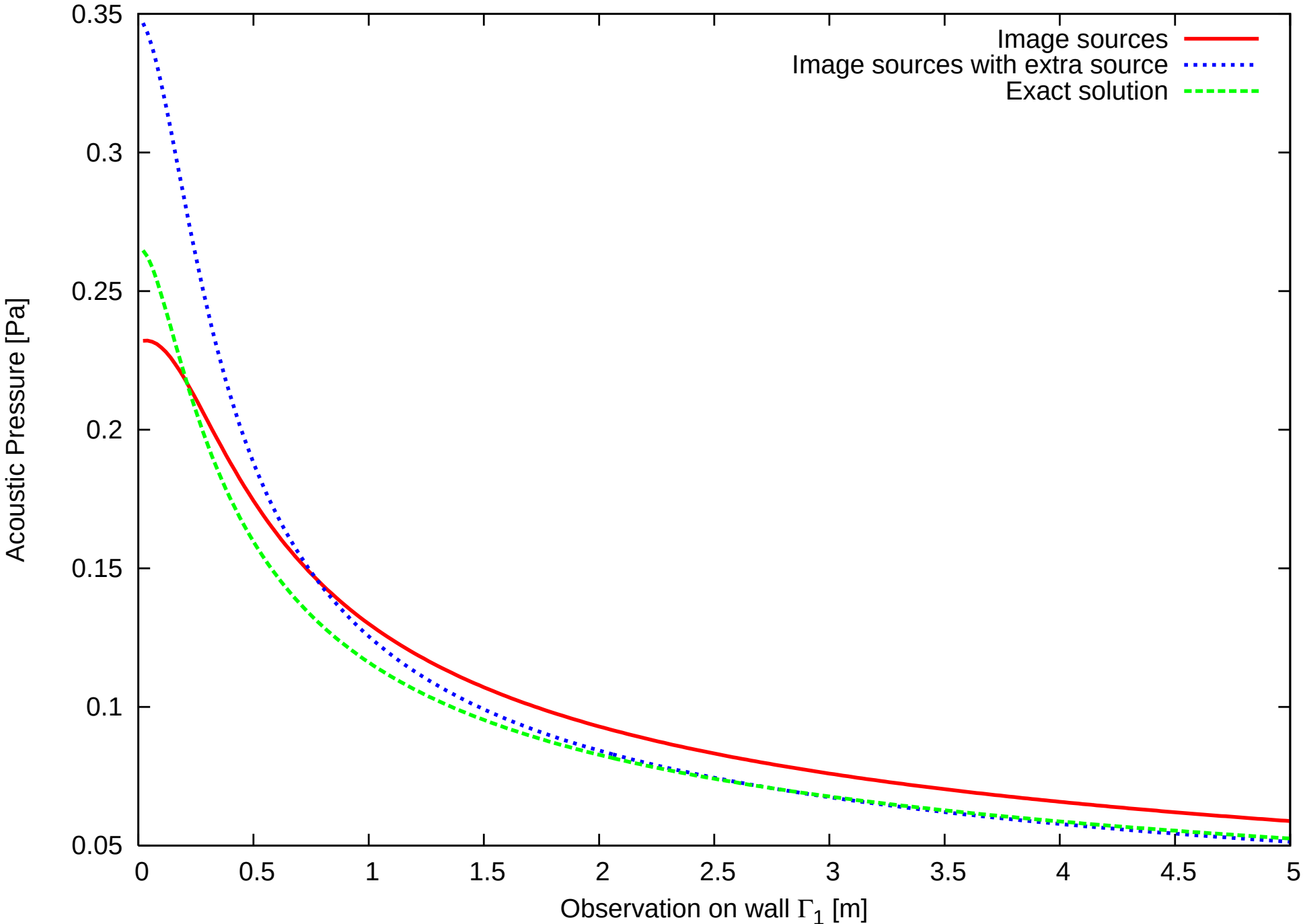
Image sources
Image sources with extra source
Exact solution
Acoustic Pressure [Pa]
0.35
0.3
0.25
0.2
0.15
0.1
0.05
0
0.5
1
1.5
2
2.5
3
3.5
4
4.5
5
Observation on wall Γ_1 [m]